JON STEEN PETERSEN

The Directional Solidification of Silicate melts: Crystallization Kinetics and Macrosegregation

ABSTRACT. *Textures and compositional variations of minerals in the contact-zone of a plutonic magma body show that solidification occurs under continuously changing conditions. Changes in crystal morphology reflect successive stages of supercooling in the contact-zone, where initial thermal supercooling is followed by the sequential increase and decrease of constitutional supercooling. Unidirectional, columnar growth ceases with the eventual elimination of constitutional supercooling and is succeeded by the formation of cumulitic – equigranular rocks. Compositional variations in the solid products reflect competitive growth kinetics in a plane front solidification contion, and are similar to variations observed in many rhythmic layered rocks. As the thermal conditions favour heterogeneous nucleation and growth of crystals that are attached to the solidification front, a chain nucleation and growth mechanism is predicted that produces regular solid interfaces towards the liquid, capable of creating both rhythmic compositional variations and steady state solidification. Layering and other planar features thus become solidification isochrons. Differentiation of the solid product is related to the rate of advance of the solidification front. Rapid advance of the interface creates differentiated products because solute accumulation cannot be removed. A slowly advancing interface may allow effective adcumulus solidification, and thus preserve primitive compositions.*

The analysis of dynamic solute redistribution during solidification bears analogy with processes of macrosegregation in metal castings. Notable features include the formation of negative and positive segregation in the lower and the upper portions of a single charge, respectively. The formation of regular compositional reversals, without relation to influx of new melt batches, emphasizes the potential of macrosegregation theory for the solution of important petrologic problems.

Department of Geology, University of Aarhus, Denmark

1. Introduction

The transformation of liquid magma into a solid product is a complicated process that involves rearrangement of liquid molecules into stable nuclei, transport of constituent elements to the nucleation site and removal of latent heat of crystallization from the growing phase. Each of

these processes may be a limiting factor for the solidification and affect the resulting product (Kirkpatrick, 1975). As the solid product is usually an aggregate of different mineral species, its overall composition will also depend on the rate of segregation of the individual phases during solidification. In order to solve the problems of magma solidification, therefore, knowledge of the rate limiting factor at any stage of the solidification is essential. Although information about stable phase assemblages allows prediction of possible differentiation paths, important restrictions exist because solidification conditions change continuously during cooling. The analysis of crystallization kinetics, which permit prediction of some effects of changing rate-controlling factors, is essential to the understanding of dynamic magma solidification processes.

Equilibrium phase relations are generally used to determine the stable solid phase assemblage of a given liquid, or the relative amounts of the constituent phases for a given temperature and pressure, (e.g. Morse, 1980). Natural rocks, however, often are not equilibrium assemblages because 1) their phase assemblages do not correspond to any reasonable source liquid (e.g. monomineralic rocks), 2) they represent disequilibrium assemblages (e.g. certain porphyritic rocks) or 3) their compositional variations are too rapid to be accounted for by changing bulk liquid compositions (e.g. rhythmic layered rocks; see review by Irvine, 1979). For all these cases, differential segregation of the constituent phases is inferred, and was traditionally considered to result mainly from physical processes of sorting such as gravity induced crystal settling (e.g. Hess, 1938; Wager & Brown, 1967) or fluid flow differentiation (Baragar, 1960; Bhattacharji & Smith, 1964; Komar, 1972). Recently, also kinetic factors have been emphasized as a prime source for fractionation during crystallization (McBirney & Noyes, 1979), the segregation being essentially chemical, caused by competitive nucleation and different growth rates in a static melt environment.

The kinetics relating to solidification of silicate melts have generated considerable interest in the latest decade (Lasaga & Kirkpatrick, 1981). Experimental studies on the crystallization of single phases have produced abundant data on nucleation and growth properties of individual minerals (Lofgren, 1974a, 1974b; Lofgren & Gooley, 1977; Donaldson, 1976; Fenn, 1977) whereas natural or synthetic rock melts have provided data on multiphase systems (Lofgren et al., 1974; Donaldson et al., 1975; Usselmann et al., 1975; Walker et al., 1976; Lofgren, 1977, 1983; Grove & Walker, 1977; Swanson, 1977; Grove, 1978; Grove & Beaty, 1980; Schiffmann & Lofgren, 1982). These recent studies were preceeded by

Harker (1909) who emphasized many aspects of crystallization kinetics, such as nucleation and growth control, influence of supercooling and faceted versus non-faceted growth. His contribution though remarkably perceptive, was overshadowed by the concept of equilibrium crystallization, and never gained the influence on petrological research it deserved.

A major problem in the application of many kinetic data to petrogenetic modeling of natural rocks is the complexity of the solidification geometry and the possible influence of fluid flow. In this respect, the study of directionally solidified rocks offers a unique opportunity to quantify some aspects of cooling and solute redistribution at a solid-liquid interface. In these rocks the product solidified sequentially along a lateral axis, thus, the diffusion problem is well defined.

Recognition of directionally solidified, natural rocks as a key to the understanding of magmatic processes was brought to prominence with the discovery and characterization of the Willow Lake layering (Poldervaart & Taubeneck, 1959; Taubeneck & Poldervaart, 1960). Later, similar features were discovered along the margins of minor intrusions in the US-Cordillera (Moore & Lockwood, 1973) and elsewhere. Perpendicular feldspars in the border zone of the Skaergaard intrusion, E. Greenland (Wager & Deer, 1939, Wager & Brown, 1967), are other examples of directional solidification, as are the spectacular harrisitic olivines and pyroxenes of the Rhum ultramafic complex (Brown, 1956; Wadsworth, 1960). Some dikes occasionally show elongated growth normal to the borders (Platten & Watterson, 1969; Drever & Johnston, 1972) as do many pegmatitic occurrences (Jahns & Tuttle, 1963). A link to the pegmatitic structures can be found in the remarkable layering and directional solidification textures recently described from granitic complexes associated with the Climax and Henderson Mo-ore bodies in Colorado (Shannon et al., 1982). Morphologically similar mineral textures have also been observed in rapidly chilled volcanic rocks such as the borders of pillow lavas (Bryan, 1972), in the spinifex-textured komatiites (Nesbitt, 1971; Donaldson, 1983) and in lunar materials (e.g. Donaldson et al., 1977).

A remarkable sequence of comb-textured rocks has been discovered recently along the contact of the lardalite nepheline-syenite complex, the Oslo Province, (Petersen, 1978a, 1978b, 1985). These form a 2-10m wide, marginal facies, with branching, dendritic minerals oriented normal to the contact and display compositional variations which include complementary phase-layering, within-layer compositional banding, columnar, monophase precipitation and gradual transition from columnar, comb-textured rocks to laminar, porphyritic varieties. Beyond

these contact zones, the interior pluton consists of extremely coarse grained, cumulitic rocks with alkali feldspar – nepheline rich outer parts and increasingly olivine – pyroxene rich inner parts with a complete, gradational transition between these extremes (Table 2 in Petersen, 1978b). This compositional variation is reverse to that of the contact zones and clearly requires a different explanation than simple prograde fractionation in a decreasing temperature regime. The range of textures and compositional variations of the lardalite complex will provide the background for the present study of directional solidification and implications for compositional variations and macrosegregation of solidifying, granular or cumulus textured magmas.

2. Columnar solidification

2.1 General setting of comb-layered rocks

The contact zones of the Lardalite intrusion exhibit directional dendritic growth of olivine (Fo_{61}), Ca-pyroxene ($En_{40}Fs_{12}Wo_{48}$), ternary feldspars ($An_{16}Ab_{75}Or_8$ to $An_7Ab_{63}Or_{30}$), nepheline and Fe-Ti oxides. These minerals appear sequentially in the contact zones from the border towards the interior. Dendritic olivines and Fe-Ti oxides are enriched in the marginal facies with alkali feldspar, Ca-pyroxene and nepheline successively appearing inward. There is, however, a wide overlap in the appearance of the feldspars and pyroxene as indicated in Fig. 1.

The crystal shape varies systematically from the margin towards the interior; dendritic varieties of the major phases are gradually succeeded by faceted ones. The changes in phase assemblage and crystal shape clearly indicate that the conditions for formation of dendritic versus faceted crystal shapes are distinct for the different phases; some phases grow with euhedral shapes when others possess highly irregular dendritic shapes.

In addition to the perpendicular, dendritic crystal shapes, the contact zones possess conspicuous *compositional layerings* normal to growth which include changing phase assemblages as well as modal fluctuations within single layers. Well defined layers of dendritic feldspar or nepheline alternate with layers of curved, dendritic Ca-pyroxene, creating a type-1 layering (Petersen, 1985). Boundaries between successive layers of this type may be sharp or gradational (Fig. 2A). Another type of compositional banding is produced by periodic variations in the amount of interdendritic material along planes normal to growth direction. This

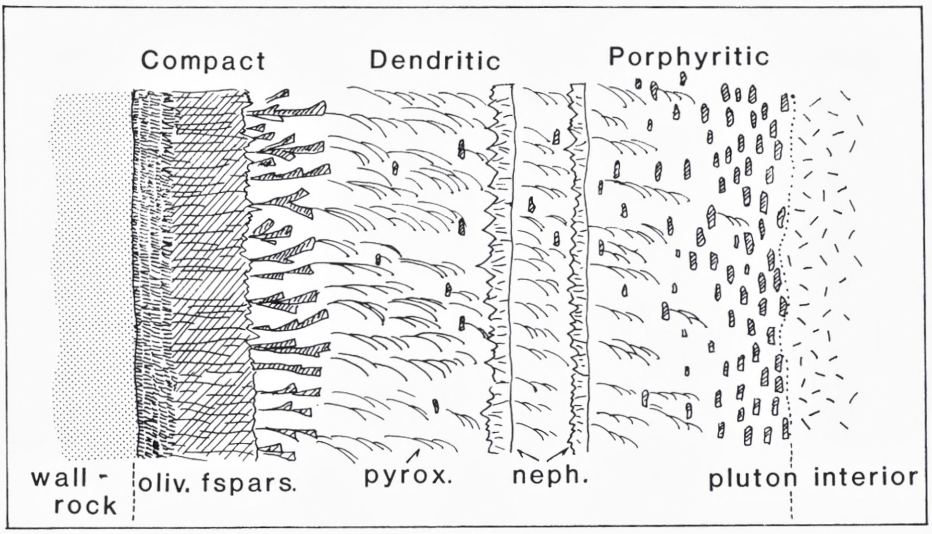

Fig. 1. Schematic cross section, showing major features of the lardalite contact zones. A marginal, olivine-rich dendrite zone is succeeded by compact and dendritic feldspar zones, which in turn are followed by dendritic pyroxene- and nepheline-rich zones. Porphyritic textures dominate the innermost portion towards the cumulus-textured pluton interior.

creates a compositional layering which typically fluctuates about constant composition and is termed type-2 layering (Fig. 2B).

Because of the large compositional variations, including some nearly monomineralic layers, average compositions of the contact zones can not be accurate estimates of the initial magma composition. Compositional variations of the individual minerals do, however, provide valuable information on the nature of the source liquid composition during solidification.

2.2 Crystal morphologies: feldspars

Ternary feldspars are the only minerals to have dendritic morphologies almost throughout the entire width of the contact zones, and also display the most diverse compositional and textural variations. For this reason, the ternary feldspars are the most useful for the study of the solidification conditions throughout the contact-zone formation.

The feldspars appear in four principal morphologies in the contact zones. Three of these are columnar with their longest crystallographic axis directed normal to the contact and the assumed solidification front, while the fourth consists of elongate, flattened and occasionally rhomb-

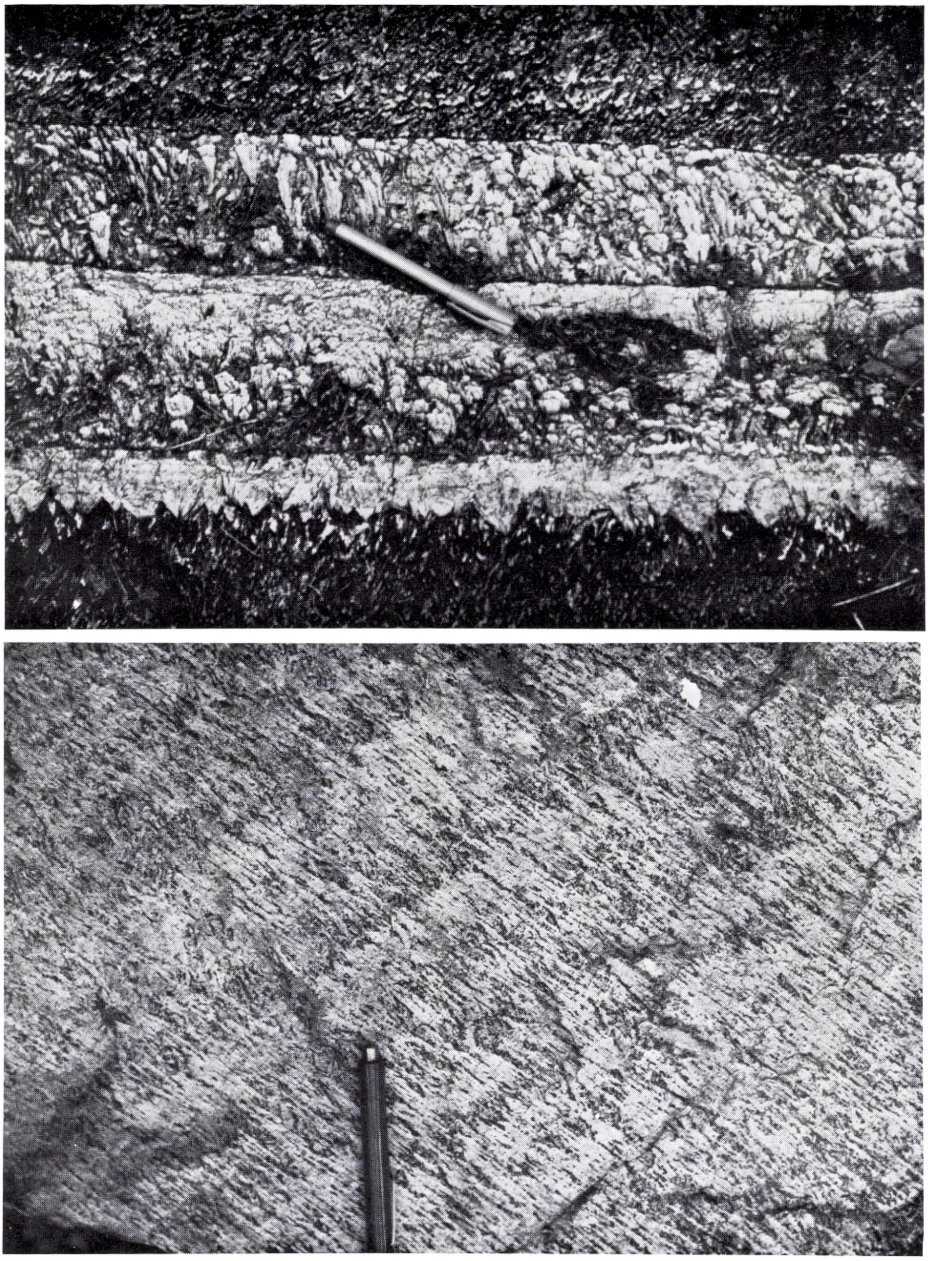

Fig. 2. A) Complementary phase layering. Dendritic pyroxene is succeeded by dendritic feldspars that gradually widen out to form compact layers. The upper boundaries of the feldspar layers are sharp whereas gradual transitions characterize the upper pyroxene boundaries. Growth is towards the upper part of the photo.
B) Compositional banding in columnar-dendritic feldspar layer. Compositional fluctuations mark small changes in steady-state solidification. Growth direction towards lower right corner.

shaped phenocrysts with their longest axis parallel to the contact. The feldspar occurrences have been subdivided into the following zones: 1) picritic rim-zone; 2) monomineralic, columnar feldspar zones, 3) dendritic feldspar zones, and finally 4) porphyritic feldspar zones (Petersen, 1985).

Picritic rim-zone feldspars are low-angle branching or curving dendrites which expand in the growth direction. Universal-Stage observations indicate that the principal elongation is parallel to the optic z-axis and therefore normal to the 010 plane. The extinction of these feldspars is undulatory, sweeping across the subgrain upon rotation and parallel to the length of the crystal. Individual subgrains are separated by slightly off set extinction positions. Polysynthetic twinning is abundant, particularly in the transverse direction, and follows the albite-law (Fig. 3). Minor domains of pericline twins follow the longitudinal direction. The distinctly curved appearance of the transverse polysynthetic twins indicates that the undulous extinction across individual dendrite branches is related to curved lattice planes, which are disrupted at neighbouring subgrain boundaries. The slightly irregular, fan-shaped dendrites of the rim zone typically measure 10-20mm and their compositions cluster around $An_{16}Ab_{75}Or_9$.

Monomineralic feldspar zones occur at different levels in the contact zones. In one such zone, near the external contact of the pluton, columnar textured feldspar has developed into a more than 2 m wide, compact layer. The feldspars within this zone are elongated perpendicular to the contact and constitute a cellular substructure. Within this substructure numerous, minor subgrains possess almost identical orientations. Optic z-directions are parallel to the principal elongation; the maximum growth direction is therefore normal to the 010 plane. Thin sections cut parallel to the columnar fabric show that the subgrain boundaries form arrays of extinction discontinuities, which divide the aggregate into parallel lamellae. Extinction sweeps simultaneously from one side of the subgrain to the other (Fig. 4A). This shingle-like texture is identical to lineage structures which are well known from unilaterally solidified metals (Buerger, 1934), and are presumably caused by accumulated dislocations along subgrain boundaries during rapid, unilateral solidification (Chalmers, 1964). Within individual subgrains of this class of feldspar, the curved nature of the lattice is revealed by a systematic change in the orientation of the optic axes across the width of a single grain, typically by 5-10° but up to 20-25° (Petersen, 1985). This is equivalent to that exposed by the curved, transverse Ab-twins in the picrite-zone feldspars.

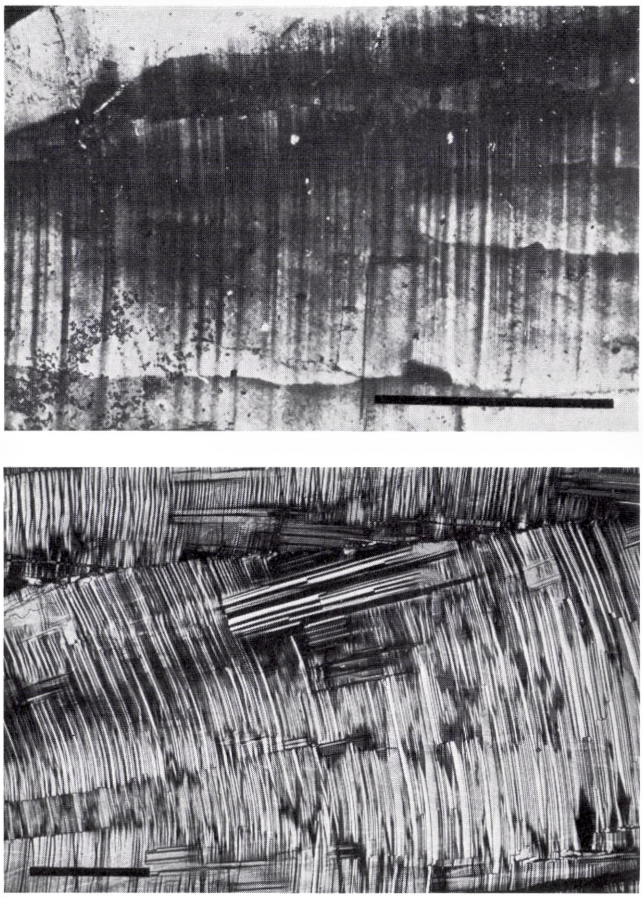

Fig. 3. A) Transverse, polysynthetic albite-twins in marginal picrite-zone feldspars. Twin plane curvature reflects curved lattice planes of the host feldspar. Growth direction towards right. Scale bars are 0.5 mm.
B) Synthetic reproduction of the curved, polysynthetic twins in feldspar-analogue material (Suberic acid). The crystals were grown directionally in high supercooling before quenching and formation of martensitic twins. (Both albite and pericline law twins).

Thin sections cut normal to the main growth direction reveal a cellular substructure with rhomb-shaped subgrain patterns of 0.7 × 1 mm and a spectacular, plaited, mesoscopic, mosaic structure (Fig. 5). Nearly identical orientation of the individual subgrains makes cleavage surfaces appear continuous like a huge single crystal and only the slightly curved appearance of each subgrain makes it distinguisable from its neighbour. The plaited mosaic structure represents two symmetrically arranged orientations divided by a coherent interface. This interface formed during primary growth by the continuous adjustment of neighbouring cell colonies into a minimum-energy boundary configuration such as twin planes as shown by Universal-Stage studies (Petersen, 1985). The rhomb-shaped pattern is a result of the anisotropic lattice properties of the monoclinic feldspars compared to the honeycomb-shaped cell

boundaries observed in many directionally solidified metallic compounds which possess isotropic, non-faceted surface properties (Buerger, 1934; Rutter & Chalmers, 1953).

The inner two-thirds of the border zones are comprised of several varieties of dendritic feldspar morphologies. With the exception of a few compact, cellular feldspars in the monomineralic zones, the dendrites in the inner parts are generally columnar with a finite spacing. The interdendritic material is usually fine grained, equigranular aggregates of complementary phases to the dendritic mineral.

Two principal dendrite types can be distinguised in this part of the contact zone. One type consist of columnar, non-branching feldspars, with constant or nearly constant spacing and orientation perpendicular to the contact or previous phase-layer contact (Fig. 6). The other, gener-

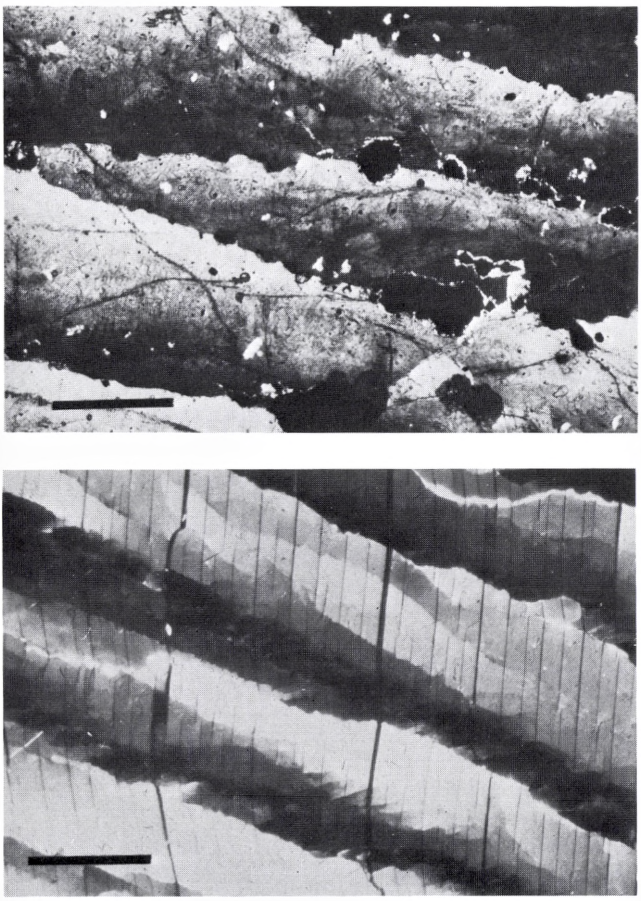

Fig. 4. A) Lineage textures in the compact feldspar zone. The shingle-like texture is due to the undulose extinction of curved lattice planes and arrays of grain bondary misfits. Growth direction towards the left. Bar 0.5 mm. B) Synthetic shingle texture in feldspar analogue materials, produced at moderate cooling rate. The structure is formed during growth by the advancement and reproduction of low-angle lattice misfits (lineage structures).

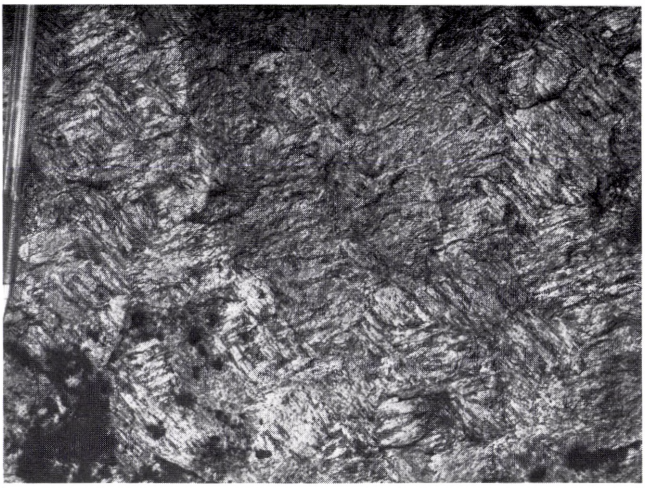

Fig. 5. Plaited structure in compact feldspars viewed normal to the main growth direction. The structure reveals a regular arrangement of subgrains or cell colonies along two dominant directions, controlled by the crystallographic properties of the growing phase.

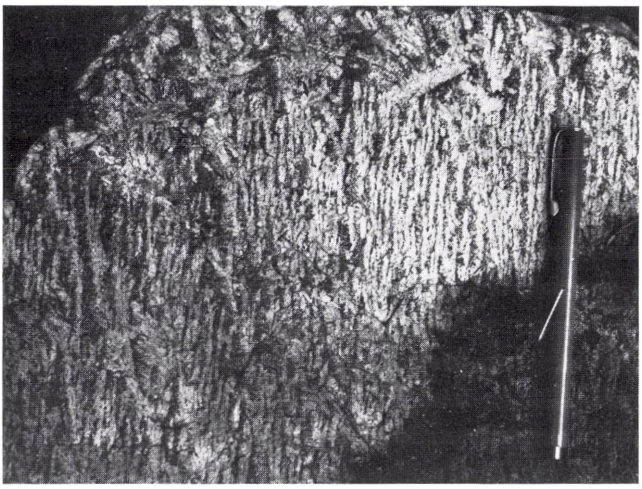

Fig. 6. Columnar-dendritic feldspars with constant spacing, indicating steady-state, diffusion controlled growth.

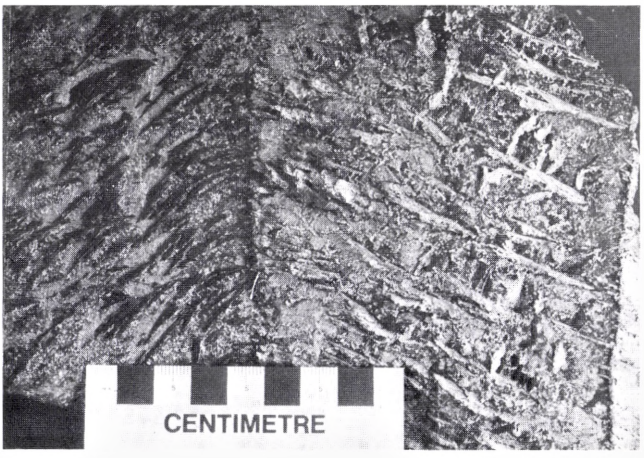

Fig. 7. Faceted feldspar dendrites have their maximum elongation deflected from the perpendicular direction to the contact. Second-arm branching compensates for the wide dendrite spacing and show maximum elongation parallel to the isotherms.

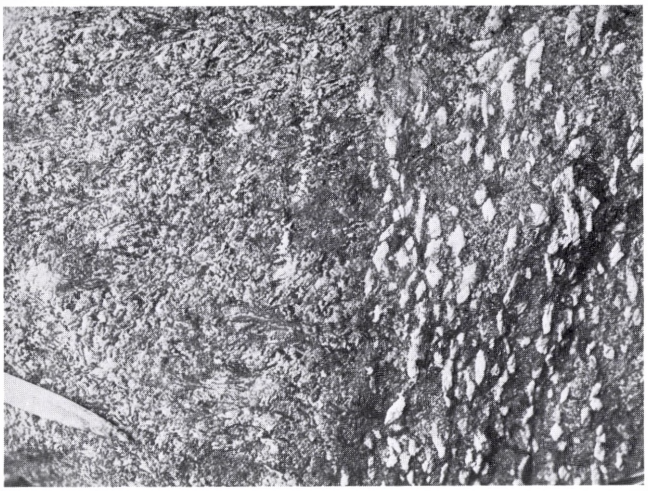

Fig. 8. Laminar textures from the inner contact zones are produced by the parallel orientation of euhedral feldspar phenocrysts with their maximum elongation parallel to the isotherms and towards the viewer.

ally occurring further inwards, is more widely spaced and oriented with the maximum elongation at a finite angle to the contact-normal direction (Fig. 7). Because of the wide spacing of these non-orthogonal dendrites, second arm branching is occasionally developed with a maximum elongation along the cooling front instead of normal to it. This texture marks a transition to the innermost zone, where feldspar phenocrysts with lamellar textures are oriented parallel to the cooling front.

The innermost portions of the contact zones are distinctly porphyritic and consist of euhedral, rhombshaped feldspar phenocrysts of 2-4 cm length set in a fine- to medium-grained matrix of olivine, pyroxene, nepheline, and biotite. The proportions of the matrix phases may vary highly resulting in ultramafic to foyaitic matrix compositions. The feldspars show consistent, parallel orientations with their longest axis parallel to the contacts and imprint a pronounced laminar textural fabric to the rock (Fig. 8).

Dendritic pyroxene and nepheline often nucleate and grow on the larger feldspar facets, indicating that substantial constitutional supercooling gradients exist in the matrix liquid. This in turn, suggests that deposition of the feldspars was not a result of gravitative settling or fluid flow along the solidification front but rather precipitation in a static boundary layer where conditions for constitutional supercooling persisted only for pyroxene and nepheline; feldspar crystallization was near liquidus conditions. Supercooling is equivalent to supersaturation in this respect; therefore the contrasting mineralogy can be caused by supersaturation rather than supercooling in the boundary layer.

Olivines

Dendritic olivines occur exclusively in the outermost portion of the contact zones, the picritic rim-zone. These olivine dendrites are fairly short (2 × 6 mm) and display irregular bifurcation, mainly as low-angle, non-crystallographic branching in the preferred growth direction. Complex intergrowths occur primarily with Fe-Ti oxides. The co-existing feldspars tend to form isolated grains, with strongly embayed boundaries towards the olivine-oxide aggregates.

The textural relations show that the olivines transgress and overgrow the Fe-Ti oxides, while the feldspars in turn partly transgress the olivines (Fig. 9). Because of the unidirectional solidification texture, the clear separation of feldspar and olivine-oxide dendrites indicates that the former cannot have formed during subsequent, interstitial growth, but must have grown simultaneously with plagioclase feldspar. Plagioclase dendrites possibly had a higher growth-rate and thus, could engulf growing olivine dendrites.

In the remaining parts of the contact zones, olivine occurs exclusively as minor, stubby crystals, generally as part of the fine grained, interdendritic matrix and often as clustered or glomerophyric aggregates.

Pyroxenes

Pyroxenes are absent in the marginal olivine-dendritic picrite zone, but are abundant in the other portions of the contact zone. Almost exclusively the pyroxenes form curved, open-dendritic crystals of 2 to 150 mm length, invariably trending inwards-downwards towards the center of

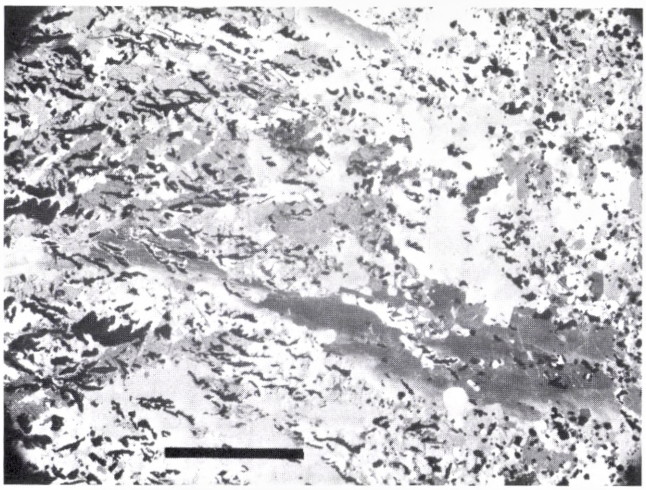

Fig. 9. Feldspar – olivine – Fe-Ti-oxide dendrites from the picrite zone show complex intergrowth textures. The textural relations suggest that the oxides preceed olivine and feldspar dendrites, which apparently grew simultaneously, side by side. Dark gray phase is plagioclase; white is olivine. Bar measures 1 mm.

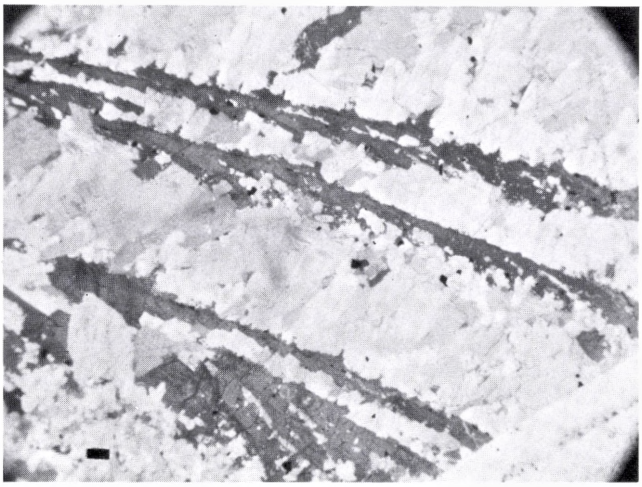

Fig. 10. Curved dendritic pyroxenes with low-angle, non-crystallographic branching along growth direction. The scale measures 1 mm.

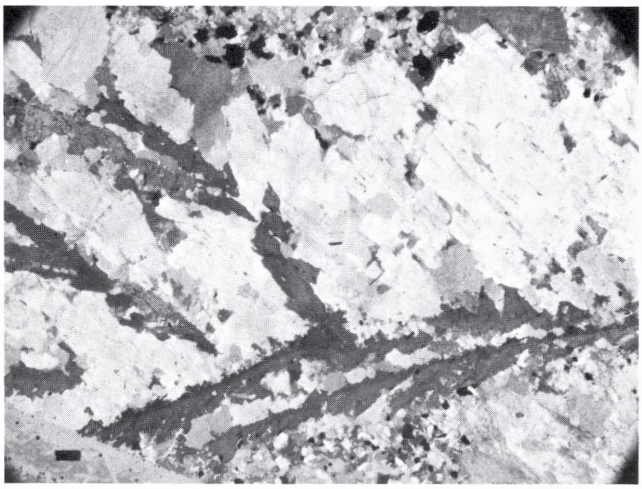

Fig. 11. Secondary nucleation of pyroxene on dendrites whose main elongation is at a low angle to the heat flow. White minerals are compact-dendritic nephelines with their growth directed towards the maximum heat flow. Bar-scale 1 mm.

the pluton (Fig. 14). Two broad types of bifurcation are present. One type shows continuous low-angle branching along the growth direction, that is partly related to the curved growth as it develops only on the concave side of the crystal (Fig. 10). The other type of bifurcation appears when the curved crystal reaches a maximum deviation from the perpendicular direction to the cooling front. In this case, subsequent branching occurs on the convex side of the crystal, initially perpendicular to the cooling front, but eventually curving (Fig. 11). This creates a chain of equally curved pyroxenes growing at large towards the cooling front (Fig. 13). These chains may actually constitute a single, continuous

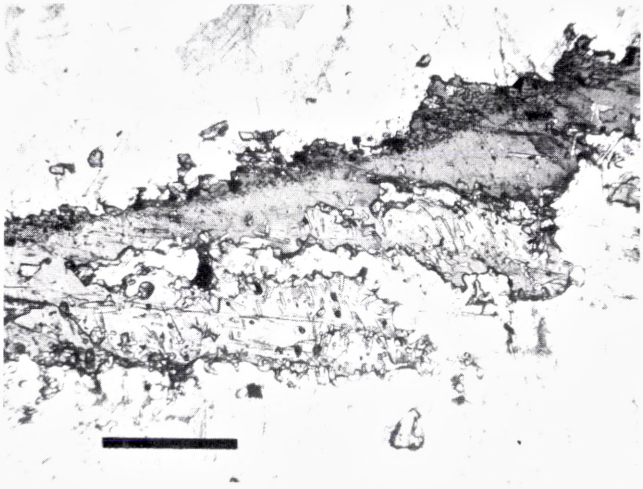

Fig. 12. Minor apatite needles, included in the pyroxene dendrites, show consistent, parallel orientations. The apatite crystals have their maximum elongation parallel to the isotherms like the laminar pyroxenes and feldspars in Fig. 16. Bar is 1 mm.

crystal for several meters, although the trace of an individual stem is difficult to verify. The curvature may be steep, up to 80° of a circle with a radius of 3-4 cm, or be very gentle.

The pyroxenes form exclusively open dendrites with appreciable amounts of interdendritic materials, mainly consisting of complimentary phases to the pyroxenes such as feldspar, nepheline, olivine, and biotite. In sections normal to the maximum growth direction, some degree of lateral spreading occurs and the curved-dendritic structure may grow into a horizontally elongated, fan-shaped sheet. This sheet has a slightly convex upper surface and a ragged multibranched lower boundary.

Euhedral pyroxenes occur only in the innermost portion of the contact zones and often together with euhedral feldspar phenocrysts. These pyroxenes are oriented with their longest axis parallel to the cooling front. Nepheline is the only dendritic phase in this part and exhibits curved branching and compact, fan-spherulitic morphologies (Fig. 16).

Abundant minute, needle-shaped apatite crystals are included in most dendritic pyroxenes. The regular orientation of these apatite crystals suggests that they were continuously precipitating along a faceted interface of the growing pyroxene and constitute an important clue to the growth mechanism of the pyroxenes. Apatites included in the interior pyroxene stems are oriented parallel with their long axis normal to the maximum growth direction of the pyroxene (Fig. 12), whereas along the margin of the pyroxenes apatite needles are aligned parallel to the surface, suggesting a later formation when facets were formed also during

lateral growth. These apatites formed as a result of local supersaturation of P_2O_5 in the liquid boundary-layer ahead of the growing pyroxenes, where residual components were accumulated. Surprisingly, similar amounts of apatite crystals are never encountered in feldspar dendrites formed simultaneously with the pyroxene dendrites. It indicates that important differences exist in the diffusive boundary layer adjacent to the different minerals.

Nepheline

Nepheline occurs in the innermost two-thirds of the contact zones, and gradually increase in abundance towards the center. The primary morphology of this phase is compact spherulitic with multiple low-angle branching and widening in growth direction, generally normal to the contact and overall cooling front.

Compact spherulitic and columnar dendritic nephelines characteristically nucleate on the upper surface of earlier dendrites or phenocrysts and in particular, on the convex side of curved-dendritic pyroxenes. These relationships imply a relatively late formation. In the inner feldspar-porphyritic and laminar-textured zones abundant growth of dendritic nepheline towards the magma interior, i.e. normal to the contact and the lamination fabric, indicate a prominent supercooling/supersaturation gradient. No textural evidence of this gradient is recorded by the feldspar morphology (Fig. 15).

Nepheline produces compact monomineralic layers, due to the trans-

Fig. 13. Dendritic pyroxenes with repeated nucleation along the growth direction.

Fig. 14. Ca-pyroxenes with typical, curved dendritic appearance. White crystals are nephelines growing directionally on the upper part of the pyroxenes (see Fig. 11 for petrographic appearance.

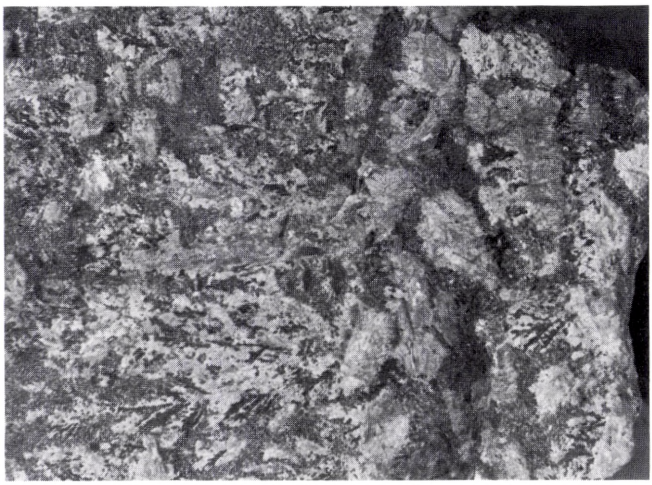

Fig. 15. Dendritic pyroxenes and nephelines in a feldspar porphyric zone. Nepheline is white, feldspar gray and pyroxene black. The feldspar phenocrysts measure 1-2 cm.

Fig. 16. Curved nepheline dendrites in a zone where pyroxenes and feldspars form faceted phenocrysts.

gressive nature of its growth. Transitional zones where cellular nepheline increases gradually at the expence of typically open-dendritic pyroxene ultimately leading into compact Ne-layers, 2-40 cm wide, are occasionally found. A contact-perpendicular cellular fabric, similar to the compact feldspar zones previously described, is formed in these layers. Unlike the feldspar zones, very few oxide or other inclusions are recorded in the dendritic nepheline.

There is an interesting periodic nature in some of these compact nepheline layers. In one example three consecutive layers of compact nepheline, interlayered by dendritic pyroxene, systematically increase in width along the growth direction. The width of the nepheline layers increases from 1.5 cm to 4 and further to 11 cm while the intervening, open dendritic pyroxene zones measure 20 cm, 40 cm and 64 cm respectively. The intervening zones are remarkably homogeneous in composition and contain about 10% vol. pyroxene. This particular three-layer zone can be traced for at least 3 km along the contact which shows its strongly pervasive nature.

2.3 Mineral compositions

Chemical compositions of the dendritic minerals were determined by electron microprobe analysis using energy-dispersive methods (Petersen, 1985). Preliminary results are summarized in Figs. 17 and 18, which show the analyses of felsic and mafic phases respectively in the three major dendrite zones.

Exsolution into Na- and K-rich components forms a very fine, string-antiperthite, potash feldspar being subordinate to albite. A coarse segregation into a K-rich and a Na-rich feldspar is apparent along the margins of mesoscopic subgrain cells (Fig. 19a). This segregation is possibly a primary growth feature and the result of cellular solidification in which the subordinate, K-rich feldspar co-precipitated as an intercellular matrix, encouraged by the rejection of solute at the cellular front. Lofgren & Gooley (1977) experimentally produced similar intergrowth textures by growth from the melt (Fig. 19b). The process is somewhat analogous to the growth of non-coupled eutectic products (Elliott, 1977). An origin by structurally controlled, solid-state segregation is, however, also possible (Petersen, 1985).

Na and K content of the feldspar increase and the Ca content decreases, with increasing distance from the contact of the pluton. Compositions of rim-zone feldspars cluster about a common value while feldspars from the inner zones show increasingly Ca-poor compositions

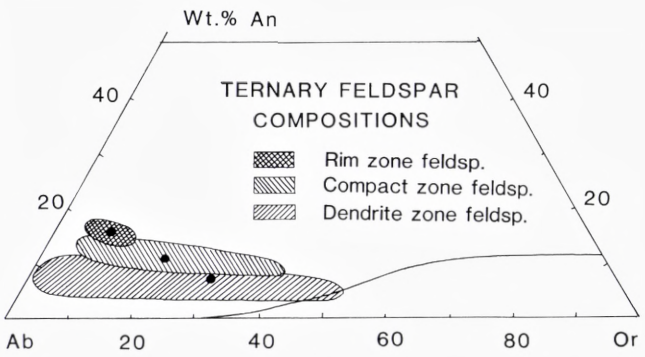

Fig. 17. Composition of dendritic feldspars from the lardalite contact zones; cross-hatched field is picrite-zone feldspars; diagonally ruled fields are compact and dendritic feldspar zones, showing decreasing Ca-content towards the pluton interior. Solid dots mark the integrated composition of each type. The spread in Na- and K-rich components can be a primary growth feature.

and a broader spread in alkali-content. The compositions of the inner dendrite feldspars suggest the existence of Na- and K-rich end members in agreement with observed antiperthitic textures.

The primary feldspar composition of each group is given by the mean value of all analyses within a group (Fig. 17). The compositional variation towards the center of the pluton is consistent with a gradually decreasing temperature. No systematic variation in Ca has been detected within individual zones. The liquidus isotherms for 5 Kbar pressure (Morse, 1970), suggest that at this pressure, solidification temperatures would be in the 900° to 780°C-interval. Actual pressures during crystallization were probably slightly lower, about 3 kbar, thus these temperatures are conservative estimates.

The compositions of dendritic pyroxenes show limited variation and consistently plot around $En_{40}Fs_{12}Wo_{48}$. The Ca-rich nature of these pyroxenes is attributable to the initial alkali-rich melt composition and the lack of substantial amounts of co-precipitating plagioclase (Morse, 1979). These compositions (Fig. 18) are significantly more enriched in Al, Ti and Mg than typical larvikite and lardalite pyroxenes (Neumann, 1976). The dendritic pyroxene compositions from the different portions of the contact zones, however, are remarkably uniform.

Dendritic olivines are Fo_{62} whereas the granular varieties of the remaining contact zones are increasingly Fe-rich to about Fo_{45}. For comparison, the range of composition in typical larvikite and lardalite olivines is $Fo_{45\text{-}30}$ and $Fo_{55\text{-}30}$ respectively (Fig. 18). The more Mg-rich compositions of the olivines of the contact zones suggest a higher temperature origin than those of the typical lardalite.

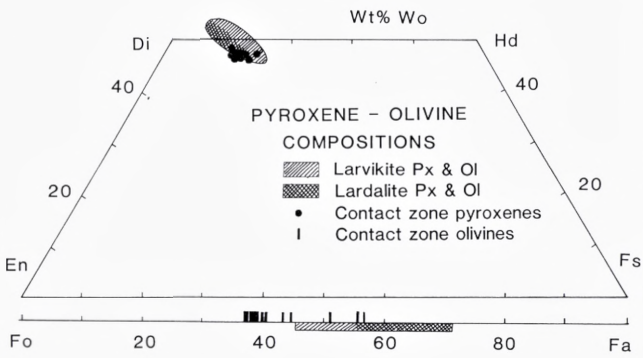

Fig. 18. Composition of dendritic pyroxenes and olivines in the lardalite contact zones, compared with average larvikite (diagonal ruling) and lardalite (cross hatched) pyroxenes and olivines. The contact zone minerals are more primitive than granular and cumulus textured minerals of the pluton interior.

Fig. 19. A) Feldspar dendrite showing segregation into Na-rich core (light) and K-rich margin (dark). Crossed nicolls; bar measures 2 mm.
B) Composite feldspar dendrite grown from synthetic ternary feldspar melt (Lofgren, pers. comm.). Separation into a K-rich (light) and Na-rich part (dark gray) is the result of growth from the melt. (backscattered electron image; total length of crystal: 6 mm.) Striking similarity with the structure of the feldspar dendrite in A) makes a related origin likely.

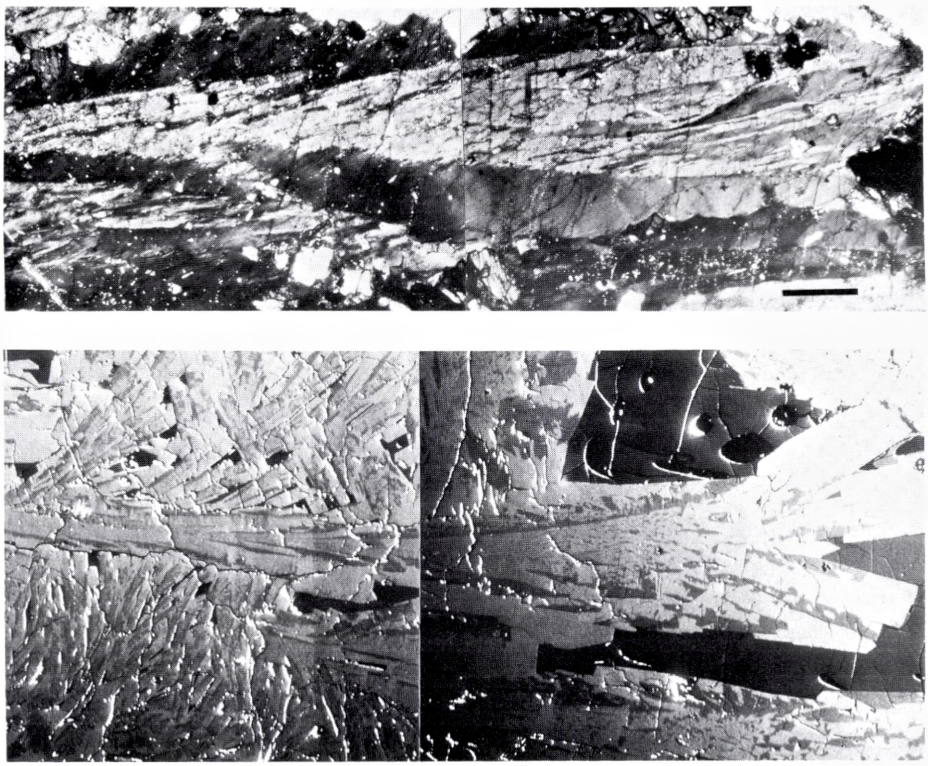

3 Discussion

3.1 Crystal morphologies

The relationship between growth morphology and solidification rate for silicate minerals has been intensively studied by experimental methods in the recent decade (Lofgren, 1974a; 1980; Kirkpatrick, 1981). These studies show that crystal morphology is strongly related to degree of supercooling/supersaturation; faceted solidification occurs with small deviations from equilibrium, whereas with increasing driving force, non-faceted and dendritic growth becomes important (Kirkpatrick, 1975, 1981). The main condition for dendrite formation is the presence of a supercooled liquid ahead of the solidification front, which makes planar interfaces unstable (Rutter & Chalmers, 1953; Jackson, 1958; Lofgren, 1974a). This condition develops when heat is extracted from the liquid faster than the rate of solidification (thermal supercooling), or when the liquidus depression of the melt attains a steeper curvature than the termal profile towards the solid-liquid interface, because of progressive solute enrichment (constitutional supercooling) (Tiller et al., 1953).

The directional solidification textures of contact zones such as the lardalite intrusion, belong to a special class of igneous textures which have been termed thermotactic (Rinne, 1926; Drever & Johnston, 1972), crescumulate (Wagner et al., 1960), Willow Lake layering (Poldervaart & Taubeneck, 1959) and comb-textures (Moore & Lockwood, 1973). Comb-texture has been adopted here because of its ungenetic connotation and purely descriptive character.

Comb-textures are the result of crystal growth from the melt (Lofgren & Donaldson, 1975). Experimental studies of feldspar and pyroxene crystallization show that directional dendritic growth with branching and bifurcating morphologies, forms readily at moderate to high degree of supercooling (Lofgren, 1980). The curved appearance of some dendrites has been suggested to result from action of fluid flow near the crystallization front (Moore & Lockwood, 1973). However, curved and spiral growth occur in environments where fluid flow is nonexistant such as the two-dimensional growth of ice-dendrites, and thus most likely are the result of purely kinetic factors.

A main characteristic of the comb-texture is nucleation on a planar crystal interface, usually along the solid wall-rock of the intrusion, but also on freely suspended crystals. Heterogeneous nucleation on a foreign substrate requires only a fraction of the constituent atoms that is necessary for a critical size nucleus to form within the melt and therefore

occurs much more readily than any other nucleation event (Shewmon, 1969). During subsequent growth after nucleation, only crystals which are oriented with their fastest growing direction along the supercooling gradient will survive the initial growth transient. Crystals in other orientations will lag behind the growth front and ultimately become extinct (Donaldson, 1977). Repeated formation of low-angle subgrain branching during progressive solidification allows continuous lattice adjustment of the growing minerals to the optimum orientation. The process of reorientation on initial crystals therefore need not involve any subsequent nucleation.

The major growth mechanisms are continuous growth and growth by layer spreading (Dowty, 1980). During continuous growth all parts of a nucleus surface constitute potential sites of atomic attachment; growth is independent of crystallographic directions. Growth by layer spreading is related to the formation of crystal facets through lateral spreading in a crystallographic plane (Kirkpatrick, 1975). This mechanism has a lower increment rate in being restricted to a certain plane, and thus it has a slower growth rate than that of continuous growth.

The formation of facets is related to the crystallographic properties of the solid and the nature of the solid-liquid transformation. Growth morphologies at small degrees of undercoolings have been successfully predicted by the application of the so-called α-factor (Jackson, 1958):

$$\alpha = M \times (\Delta H_m/kT_e) \text{ or } = M \times (\Delta S_m/k)$$

where ΔH_m is heat of fusion change; k the Boltzmann constant; T_e the melting temperature; ΔS_m entropy of fusion; and $M = \eta/\nu$, the fraction of binding in the growth plane to total binding energy, also called the anisotropy factor. The α-factor thus consists of two terms, one being related to the entropy of fusion for the particular substance (ΔS_m) and the other being related to crystallographic properties of the substance (M). This shows an important property of facet formation, since it may vary both with respect to substance and with respect to crystallographic directions.

Most metals possess low values of ΔS_m which make their α-factor less than 2, implying growth by non-faceted, rough interfaces, i.e. a continuous mechanism (Jackson, 1972). Many organic materials have values greater than 2 and thus produce faceted interfaces upon freezing (Jackson & Hunt, 1966). The α-factors of most silicates are generally well above 2, except for quartz, albite, and sanidine which have low ΔS_m-values of

0.33, 0.75 & 0.77, respectively (Carmichael et al., 1974), and therefore α-factors about 2.

A interesting example of faceted growth is the crystallization of water, because ice has an α-factor near the critical value of 2 (~ 1.97) (Jackson, 1958). Because slightly higher binding energies are associated with the basal plane, this plane possesses α-values greater than 2, whereas other crystallographic planes have lower values. At small undercoolings, where growth anisotropy is maximized, facets form only along the basal plane; dendritic growth is experienced in all other directions. Freezing under these circumstances creates large flat sheets with maximum extension along the basal plane, (i.e. dendritic growth constrained by only one facet plane). Lateral growth of ice dendrites produces a cellular texture consisting of parallel sheets (Rohatgi & Adams, 1967) that completely mimics the braided texture of the compact-zone feldspars from the lardalite intrusion (see Fig. 5).

Under conditions of extreme supercooling, feldspar and pyroxene tend to form spherulitic masses, constituting aggregates of numerous crystals which radiate away from a common center (Keith & Padden, 1963). Technically, spherulites are multicrystalline aggregates, since each needle has an independent orientation; physically, however, all needles derive from a common nucleation center and thus constitute a single unit. The radiating nature is due to the presence of a constitutionally supercooled liquid around the freely suspended nucleus and the formation of abundant low-angle non-crystallographic branching of subgrains during subsequent constrained growth (Keith & Padden, 1963).

Two major categories of spherulites are defined (Keith & Padden, 1963) as compact (massive) and open (spiky) spherulites. In compact spherulites, neighbouring subgrains touch and leave no interdendritic material whereas the open spherulites contain appreciable amounts of interdendritic material. Miller (1977) found that in highly purified, monophase systems, the formation of facets was critical for the formation of open spherulites, as opposed to compact ones. A faceting plane will, because of growth competition, ultimately become oriented parallel to the maximum growth direction, and this facet will then allow separation from the neighbouring subgrain of the spherulite (i.e. formation of an open structure).

The morphologies of feldspar and nepheline in the monomineralic zones are analogous to that of compact spherulites, except that growth is not radiating from a common nucleation center but from a common nucleation plane in a parallel fashion. Initial radiating fabrics are occa-

sionally seen but are obliterated as adjacent spherulite colonies interconnect to produce a compact, parallel-textured layer (Fig. 2A). Because of the cooling geometry with isotherms parallel to the contact and heat of crystallization being extracted through the dendrite stem, a zone of constitutional supercooling will constrain the maximum growth normal to the interface (Rutter & Chalmers, 1953).

Feldspars

The consistent orientation of feldspars in the contact zones show that maximum elongation is invariably normal to the 010 plane (Petersen, 1985). This suggests that solidification is not a continuous mechanism, as usally assumed for cellular growth, but faceted with the orientation being controlled by at least one crystallographic direction. The lack of inclusions in the central part of the feldspar dendrites indicates that maximum growth occurred in the central part of a crystal face and spread towards the edges, possibly by a spiral growth mechanism caused by screw-dislocations. Other mechanisms involve nucleation of new layers along the edges and the formation of skeletal morphologies and inclusions in the central portion of the facets (Kirkpatrick, 1981).

Gilmer (1977) presented experimental evidence which supports computer simulations of crystal growth in showing that closely packed faces are more likely to form facets because of the higher binding energy associated with such planes. More loosely packed directions on the other hand maintain a rough interface at the lowest supercooling (i.e. they have high roughening temperature). The roughening temperature indicates the supercooling necessary for a particular crystallographic direction to transform from a slow growing facet to a rough, continuously growing interface (Gilmer, 1977; Hartmann, 1982).

In feldspar, the closest packed facet-plane is the 111 plane following Voensdreght's (1983) analysis of PBC-vectors for plagioclase feldspar, using the crystal-bond concept of Hartmann-Perdock (Hartmann, 1973). The 010 plane is the most loosely packed f-face. According to Gilmer's (1977) results, but contrary to the common view, facets are likely to form initially on the most densely packed faces like 111 and proceed sequentially to the least densely packed faces like 010 in a sequence of decreasing supercooling and following the increasing roughening temperatures of various facets. This mechanism will allow the 010 plane at some stage during solidification to be the only face to maintain a high growth rate because of its relatively high atomic roughness. The com-

petetive nature of directional solidification will therefore allow only this direction to grow normal to the isotherms.

By analogy with the ice discs discussed above, the growth of a single facet, once formed, will be retarded, and ultimately become oriented normal to the fast growing direction due to the continuous competition for maximum growth rate. A single facet will restrict crystal growth in only one direction, resulting in parallel sheets with similar orientations in compact spherulites (Fig. 20A). Initially, individual sheets may show random orientations normal to the faster growth direction, but because of competitive growth, they ultimately become aligned to form a superficial sheet structure. Twin planes may allow modification of this sheet structure to form a braided texture of two or more directions as observed in the compact, columnar feldspar zones (Fig. 5).

When two facets form, growth is restricted to two directions in space. This allows formation of columnar structures which are separated by varying amounts of interdendritic materials in the growth plane (analogous to rod eutectics) (Fig. 20B). Maximum growth is largely unconstrained in the third direction which is still below its roughening temperature and accordingly oriented parallel to heat flow, i.e. perpendicular to the contact with the magma. At this stage the compact feldspar structure will grade into a columnar texture with interdendritic material becoming abundant towards the inner portion of the contact zones. This type of

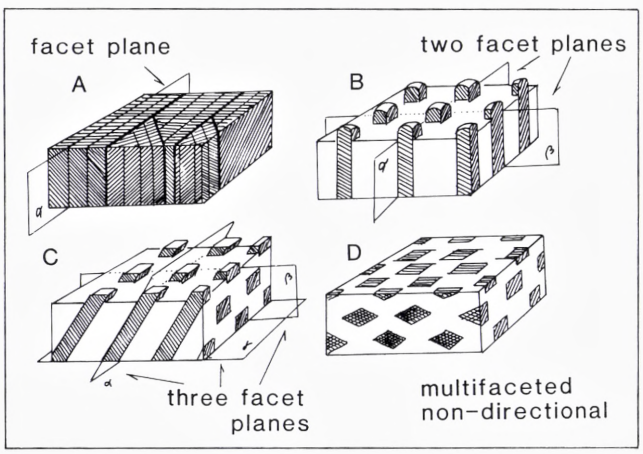

Fig. 20. Cartoon showing the effects of facets to the growth morphology of directionally solidified products. A) one facet leads to a lamellar fabric; epitaxial twin planes allow for subsequent directions which can result in a plaited structure. B) Two facets restrict growth in lateral directions and lead to columnar shapes. C) Three facets constrain growth in the third dimension, and deflects the maximum growth direction from that of maximum heat flow. C) lack of constitutional supercooling eliminate directional growth and three or more facets lead to porphyritic products with maximum elongation parallel to the isotherms (laminar textures).

growth corresponds to the open spherulitic growth of Miller (1977) and implies a second step in the direction of increasing growth anisotropy with decreasing supercooling. At least two facets are required to prevent dendrites from growing together in a transverse direction.

Growth is constrained in the third dimension when three facets form, and the maximum growth becomes directed away from the maximum heat flow direction. (Fig. 20C). The maximum growth is now pointed towards the nearest favorable crystallographic direction, as found for faceted dendritic growth in binary systems by Morris & Winegaard (1969).

The morphology is determined by the relative growth rate of the slower growing faces only when supercooling is almost totally eliminated. Under these conditions the temperatures are above the roughening temperature for all major facet planes. Maximum elongation is then parallel to the crystallographic c-direction in feldspars and parallel to the 010 plane, forming rhomb-shaped crystals typical of the lardalite interior (Fig.20D). These rhomb-shaped feldspars are dominated by crystal faces like $\bar{2}01$, 110, & 110 (Oftedahl, 1948), and growth rates for the various crystallographic directions can be ranked as $c < a < b$.

Pyroxenes

The most pronounced growth feature of the dendritic pyroxenes is clearly their curved dendritic shape. From the previous discussion it is clear that isolated dendrite stems imply faceted growth. Furthermore, the deviation of the faster growth direction from that normal to the cooling front implies that at least three facet directions control the growth. Taking the commoner facets of equilibrium shaped Ca-pyroxene as potential f-faces (Hartmann, 1982), it is likely that Ca-pyroxene forms facets in a manner slightly analogous to that of monoclinic ternary feldspars. That is, maximum density planes like 111 forms facets most readily following Gilmer (1977), while the loosely packed faces like 100 and 010 are late, and with the 001 and 110 planes as intermediate facets. Due to the competitive growth, the more rough interfaces 100 and 010 grow fast and tend to become oriented towards the maximum heat flow. Since these directions, however, are intercepted by the readily faceting 111 plane, maximum growth will become deflected at this intercept (Fig. 21). The growth thus produces an oblique directed dendrite with a planar (faceted) upper surface and a more irregular lower surface; the latter may produce secondary facets along 001 and 110 as the interdendritic growth proceeds.

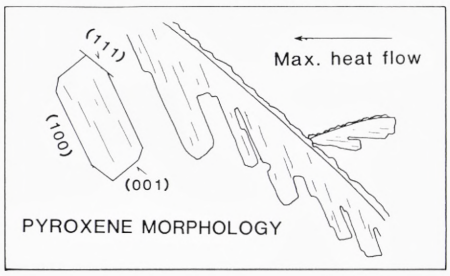

Fig. 21. Crystallization of deflected pyroxene dendrites. Intersection between the fast growing 100 and 010 directions and a facet plane (e.g. (111)) results in a deflection of the maximum elongation of the dendrite from the direction of maximum heat flow.

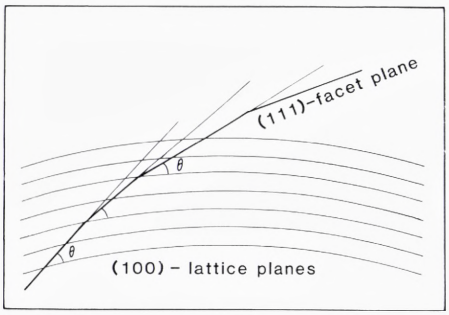

Fig. 22. Curved, external facets of pyroxene dendrites are the result of the interference between lattice-plane curvature of the fastest growing 100 direction, and the constraining facet plane 111, which gradually moves across the lattice curvature during growth and thereby leads to a curved overall shape. A curved dendritic shape thus, is the result of crystallographic factors alone.

The consistent curvature has been suggested to derive from flow of nourishing liquids past the crystallization front, imposing a compositional gradient (Lofgren & Donaldson, 1975). As realized by these authors, however, curvature is often developed in systems where flow is absent, and therefore a more general explanation is clearly wanted. The conspicuously curved lattice revealed by curved albite twins and deflected optic axes across single subgrains in the 010 plane of dendritic feldspars may contain the clue to an explanation of this phenomena.

Since the curvature along 100 is an overall lattice feature, the facet along 111 will gradually transgress upon this plane (Fig. 22). The angle θ between 100 and 111 however is a lattice constant and therefore as the transgression proceeds across the 100 plane, the 111 facet will become increasingly deflected. This leads to a systematic curvature of the resulting dendrite. Although curved dendritic growth of the analogous feldspars are more uncommon, a few examples (Fig. 23) show that the explanation also holds for feldspar. In Fig. 23 the curved nature of the 010 plane is seen from the weak differential coloring across the dendrite stem.

The above mechanism causes the pyroxenes to grow at an increasingly lower angle to maximum heat flow. When the angle of growth becomes sufficiently low, repeated nucleation occurs on the upper 111 facet, and a

new pyroxene starts growing initially perpendicular to the heat flow, in order to keep up with the continuous cooling; isotherms moving parallel to the contact. This process explains the regular, repeated nucleation seen in all the dendritic pyroxene zones (Fig. 24).

In summary, the formation of facets imposes a major control on the morphology of growing phases in supercooled conditions. This control is apparent in the sequence of crystal morphologies in the contact zones of the lardalite intrusion. The sequence of morphological types in these zones corresponds closely with that theoretically developed in a decreasing gradient of supercooling, which in turn causes a corresponding, stepwise increase in growth anisotropy (Fig. 25).

3.2 Compositional variations

Dendrite spacing

The regular spacing of dendrites in the inner dendrite zones of the lardalite intrusion, indicates steady-state growth at constant velocity. This view applies to both the open dendrite pyroxene zones and to the columnar feldspar dendrite zones. The spacing can be partly analyzed by assumming a diffusive boundary layer around each dendrite tip (Petersen, 1985). This layer has a radius of the characteristic diffusion distance; the problem of overlapping diffusion spheres is solved quantitatively in a fashion analogous to that of lamellar eutectic growth (Jackson & Hunt, 1966; Scherer & Uhlmann, 1975). When the interdendritic spacing is equal to twice the characteristic diffusion distance (Fig. 26A), lateral growth is inhibited by the equilibrium melt composition at the crystal melt interface. This is because excess solute from the interdendritic space

Fig. 23. Dendritic feldspar showing curved growth morphology. Convex, lattice planes can be recognized from the weakly discolored, transverse pattern on the feldspar stem. The crystal measures 18 cm. Secondary nucleation of pyroxene and nepheline on the upper surface tends to readjust growth towards the maximum heat flow.

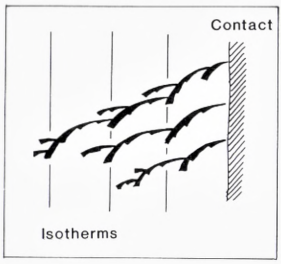

Fig. 24. Sketch of curved pyroxenes showing repeated nucleation when growth is directed almost parallel to heat-flow. Compare with Fig. 13 and 23.

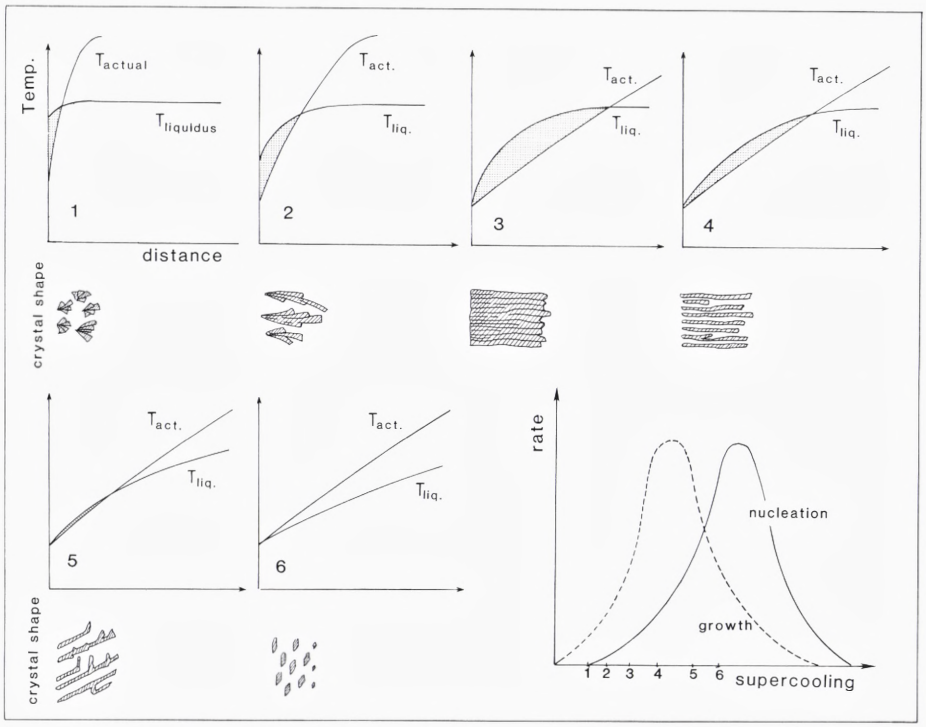

Fig. 25. Summary of growth morphologies and growth conditions for the contact zone feldspars in terms of thermal and constitutional supercooling from the margin (1) and inwards (2-6) (from Petersen, 1985). Initially high thermal supercooling result in semispherulitic crystals (1); increasing constitutional supercooling (2-3) results in directional growth. Formation of successive facets controls growth morphologies in (3-5) as thermal and constitutional supercooling decrease. In (6) the supercooling is eliminated and the crystals grow essentially parallel to the isotherms.

can be removed only in directions normal to the boundary layer. In this case, growth of the dendrite is constrained in all but one direction, and therefore, conformable to plane-front solidification.

When the interdendritic spacing is larger than twice the diffusion distance (Fig. 26B), transverse diffusion allows some lateral growth until mutually opposed diffusion spheres meet. Subsequent branching of dendrites may occur so as to adjust the solidification rate to a maximum for a given supersaturation (Flemings, 1974). In both cases, however, the process ultimately leads to unidirectional growth which is qualitatively comparable to plane-front solidification. Finally, if dendrite spacing is less than twice the diffusion distance (Fig. 26C), competitive solute enrichment occurs due to overlapping diffusion spheres. The growth of some dendrites is hindered and lags behind that of neighbouring dendrites. The situation then resembles that of case-B, where lateral growth or subsequent branching gradually eliminates transverse diffusion.

The above dendrite-spacing-regulation mechanism tends to adjust the dendrite spacing to optimum configuration for a given growth rate. Experimental evidence verifies that the spacing in cellular dendritic growth correlates with the rate of cooling rather than with the rate of motion of the isotherms (Chalmers, 1964, p. 170). This implies that growth is controlled primarily by diffusion rather than by heat transfer. Dendrite spacing is therefore, governed by the characteristic thickness of the diffusion zone around the growing dendrite as argued previously by Howarth & Mondolfo (1962).

A systematic overall decrease in the feldspar to matrix ratio is found

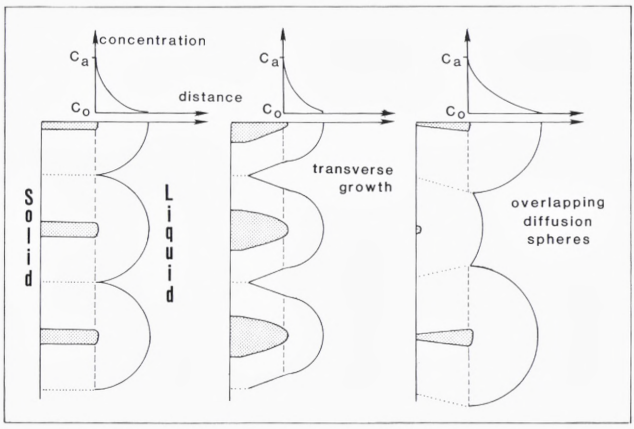

Fig. 26. Dendrite spacing regulation. Each dendrite tip acts as a source of solute, which build up in semi-spheric diffusion zones. (A) When the dendrite spacing is twice the characteristic diffusion zone, transverse growth cannot occur. In (B) is transverse growth possible until opposite diffusion spheres meet. In (C) overlapping diffusion spheres prevent growth of some dendrite stems.

from the pluton margin inwards. This suggests that the effective diffusion spheres increase in width inwards with decreasing cooling rate. Since a steady-state solidification is implied, solidification rate was diffusion controlled and the increasing diffusion spheres therefore not a result of decreasing solidification rate but rather the effect of increasing boundary layer width and less efficient removal of solute. This can happen because the convective flow velocity decreases with time or because the static diffusion zone widens as a result of increasing liquid viscosity.

Steady-state growth

Plane-front solidification has important implications for columnar-dendritic solidification if the maximum growth direction is not controlled by the interface reaction. As noted above, the solute content can be viewed as the amount of interdendritic material, which remains constant during steady-state solidification. Any change in the solidification rate, however, may result in compositional fluctuations about this constant value (Tiller et al., 1953). A change to slower growth rate momentarily reduces the solute accumulation rate and causes a temporary reduction in the solute diffusion zone. If additional branching is not developed, this reduction allows increased transverse growth of the pre-existing dendrite columns and creates a higher dendrite to matrix ratio in the growth front. The solid product will momentarily attain a lower concentration of solute (matrix) than the average melt. This imbalance results in a subsequent accumulation of solute in the solid phase until C_s again approaches steady-state composition.

For example, a steady-state dendritic solidification affected by a minor change in growth-rate from Y_1 to a slower growth rate Y_2 (Fig. 27) is accompanied by a reduction in solute accumulation. A momentary increase in dendrite width occurs, and causes the feldspar to occupy a larger volume proportion. Solute concentration in the solid product, viewed as the amount of interdendritic material along the solidification front is thereby lowered. Compared to the source liquid, this lower average solid composition renews enrichment of the solute to the boundary layer and in turn affects the dendrite to matrix ratio, which subsequently returns to the steady-state value.

The textural product of the above process may be a transverse, within-layer banding observed in some dendrite feldspar zones (Type-2 layering) (Fig. 2B). In these zones, numerous feldspar-enriched bands occur across the regularly spaced dendrite arrays and average compositions fluctuate about a constant composition.

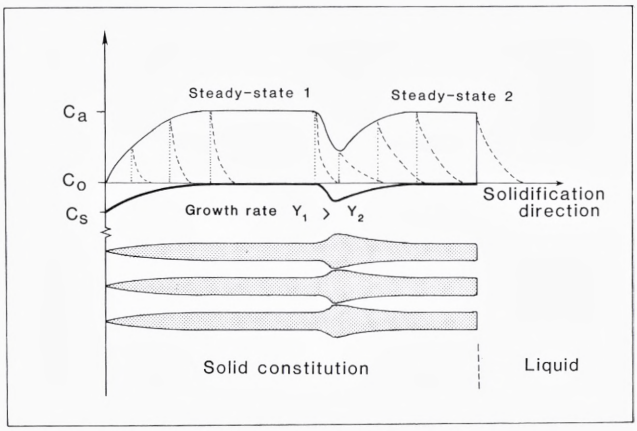

Fig. 27. Steady-state dendritic solidification with periodic changes in growth rate results in compositional fluctuation about constant composition. A sudden change from growth rate Y_1 to a slower rate Y_2 causes momentary reduction in solute content and thus a commensurate dendrite widening. This causes imbalance in the solute production which gradually forces crystallization to return to steady-state.

Complementary phase layering

Layering produced by the successive appearance of complementary phases is much more conspicuous than banding produced by slight variations in modal proportions resulting from steady-state growth of a single phase. Individual layers and intervening zones of open-dendritic or laminar-textured rocks with complementary phase layering typically have constant composition, but they may vary from polyphase dendritic to almost monomineralic. Despite their constant composition which indicates steady-state conditions these layers are not representative of bulk melt composition. Characteristics of damped oscillatory reactions are evident in the periodic nature of this layering. The nature of this periodicity suggests that complementary phase layering originates by competitive, oscillatory chemical processes. These processes may follow a nucleation-diffusion model initially proposed by Harker (1909) and recently reemphasized (McBirney & Noyes 1979), which in ideal terms, stems from the interaction of two parameters of growth with different rate properties such as e.g. heat flow and chemical diffusion.

As solidification moves from an arbitrary position x_1 to x_2, heat flow varies linearly with time and elemental diffusion varies with the square of time (McBirney & Noyes, 1979). Therefore, at the start, the depletion of constituent elements moves faster than the cooling front and prevents subsequent nucleation. When the depletion zone is ultimately overtaken by the nucleation isotherm, a new burst of nucleation and subsequent growth will occur and create a repeated appearance of single phases in a rhythmically layered, solid product.

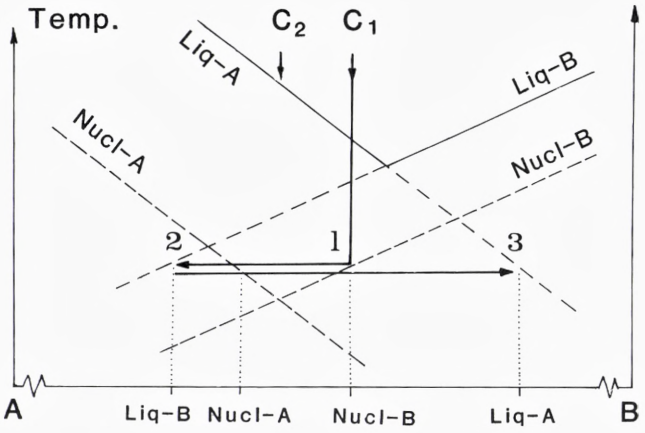

Fig. 28. (A) Complementary phase layering as a result of competetive nucleation and growth. See text for discussion.

Although intuitively satisfying there are indications that this process, at least for single phase nucleation, may reach steady-state and not oscillate (Allègre et al., 1981), unless it is triggered by an external mechanism such as the nucleation of a secondary phase. Steady-state solidification apparently does occur in the contact zones of the lardalite intrusion, since compositional variations are minor throughout most of the individual layers except for the occasional fluctuations discussed above and for conditions near the phase change, where gradual changes occur. Therefore a model is needed which allows the formation of even monomineralic products at a steady-state to become abruptly terminated and taken over by subsequent phases.

Solidification involving two complementary phases is discussed by using a simplified binary diagram (Fig. 28). The phases are stable below their respective liquidus curves, but only nucleate on the nucleation curves, which mark the necessary supercooling for stable nuclei of phase A and B respectively. In supercooled condition, the phases are stable below the extension of their respective liquidus lines.

A liquid of composition C_1 is supercooled until phase B nucleates and starts growing (Fig. 28). Assuming a broadly isothermal solidification, where latent heat of crystallization is removed through the solid phases, growth of phase-B drives the interface melt towards the left in the diagram. Depending on the size of the effective partition coefficient ($^{\star}K_D$), and the width of the static boundary layer, the composition of the solid may be very different or very similar to that of the source liquid. In the first case, the boundary-layer liquid will reach the nucleation curve for

phase A rapidly and cause coprecipitation of A. In the latter case, steady-state solidification may develop, and remain until the reservoir liquid becomes saturated with respect to phase A, due to a decrease in temperature.

If phase A has a higher growth rate than B, phase A will take over the crystallization front, since the faster growing phase will enclose grains nuclei of the slower growing phase along the solidification front and development of phase B becomes prevented in the solid. Solute redistribution during this transitional stage is complex, but after completion it conforms again with the diffusion-sphere model discussed above, and thus a planar-front solidification model. From this stage (Fig. 28(2)), B-components now accumulate in the boundary layer relative to A-components and drive its composition towards the right.

When the interface liquid passes (1), nucleation of B will occur together with the continuous growth of A, but because of the growth rate differences discussed above, this rarely affects the bondary layer composition. In ideal isothermal solidification, the boundary layer proceeds directly towards the liquidus composition at (3). When it reaches the liquidus composition, equilibrium crystallization proceeds without any trend reversals until the source melt ultimately becomes differentiated. However, if solidification is not entirely isothermal, because latent heat of crystallization is not removed effectively from the faster growing A-dendrites or the liquidus is lowered because of volatile build up, then the interface temperature may rise above the liquidus temperature at (3) and promptly prevents further growth of phase-A. Nucleation and growth of the secondary phase-B, which is still in its stability field, then substantially influences the boundary layer and reverses the compositional trend. In contrast to the previous case, this phase contact will be sharp following the isotherms, and starting a new cycle of compositional layering.

An example of this process is sketched in Fig. 29, where A may represent feldspar or nepheline and B olivine or pyroxene. For a melt composition corresponding to C_1 in Fig. 28, the layered sequence would be (1) olivine (or/pyroxene), (2) olivine (/pyroxene) *and* feldspar (/nepheline), and (3) feldspar (/nepheline), assuming a higher growth rate for feldspar (/nepheline) than for olivine (/pyroxene). This sequence duplicates the order of appearance and layering observed in the marginal picrite zone of the lardalite intrusion towards the dendritic feldspar zone as well as the nepheline – pyroxene layering of the innermost dendrite zones. A slightly different composition at C_2 (in Fig. 28) causes primary precipitation of

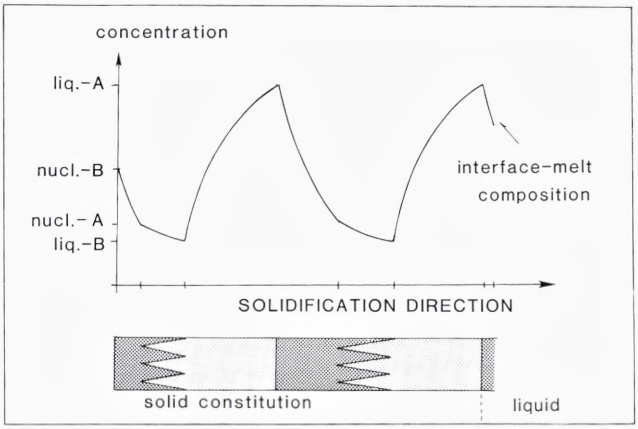

Fig. 29. Schematic relations between two complementary phases like feldspar (A) and pyroxene (B); the former is assumed to have a higher growth rate. The upper boundaries for the faster growing phase are sharp whereas the upper boundaries for the slower growing phase are gradational. Phase-relations from Fig. 28.

feldspar, which would persist to produce a monomineralic feldspar zone. The feldspar continues to grow until heat-production brings the interface temperature above the liquidus. Numerous minor inclusions of Fe-Ti oxide dendrites in parts of the outermost, columnar feldspar zone (see Fig. 6 in Petersen, 1985) may represent engulfed nuclei of co-precipitating B-phases.

4 Equigranular solidification

4.1 Introduction

In the previous sections, solidification features related to the solid-liquid transformation with a fairly simple geometry, a unilaterally propagating planar front, were emphasized. The following sections examine aspects of solidification with a non-planar front and repeated nucleation. Similar compositional variations in comb-textured and cumulus-textured rocks suggest that the mechanisms of layering are related. The gradual transition from columnar to equigranular texture with decreasing supercooling suggests that both of these textures result from nucleation and growth in a similar heat-flow environment, but with different solidification rates and mechanisms, rather than being products of completely different solidification conditions. The purpose of this section is to examine the relationship between lateral solidification and compositional variations in equigranular rocks, and to discuss some petrological consequences.

The term, equigranular, implies equal grain size and equidimensional

shapes of the constituent minerals. Its usage here is not completely accurate as the types of solidification structure with repeated nucleation discussed below may equally well produce any type of cumulus texture. The term is used, however, because it indicates an isotropic, non-directional texture as opposed to the strongly anisotropic, columnar or comb-layered products of lateral solidification discussed earlier. It is synonymous with the term, equiaxed texture, which is used in the metallurgical litterature for analogous texture patterns (Chalmers, 1964).

Equigranular solidification textures may form in a static melt when the nucleation rate is sufficiently high to cause repeated nucleation along the cooling front rather than growth of preexisting phases. This process occurs in chilled margins where the nucleation rate is maximized at high supercooling, and the growth rate is small or moderate (see Fig. 25). Equigranular textures, however, may also form at *low* supercooling, when the maximum growth direction is constrained by crystallographic factors, and directed at some angle to the direction of maximum heat flow. Nucleation of new grains on pre-existing crystals subsequently occurs so as to adjust solidification rate to keep up with the conductive heat loss through the wall rock. Despite their similar texture patterns, the conditions for the formation of the above two equigranular products are fundamentally different, and these differences become reflected in the contrasting compositional properties of the products.

As for directional solidification of dendritic and cellular products, important contributions to our understanding of unilateral solidification of granular textured products is provided by experimental studies of continuous casting processes in axisymmetrical ingots. These experiments show that systematic compositional variations occur in almost any solidification geometry (Flemings, 1974; p245). This type of variation, known to metallographers as macrosegregation, is derived mainly from the interaction of diffusive boundary layers with fluid flow in the interdendritic region, also called the mushy zone. Other mechanisms such as floating or settling of crystals or convective flow of liquid plus solid may contribute to the macrosegregation in special cases (Mehrabian, 1984).

Plutonic intrusions in a simplified sense are vast castings of silicate magmas, and are analogous to the much smaller scale metallurgical castings in which macrosegregation is important. It seems fitting therefore to examine the origin of compositional variations in plutons with respect to crystallization kinetics and macrosegregation. Compositional variations which are inconsistent with the variations expected along the liquid line of descent of the magma are particularly significant in this respect.

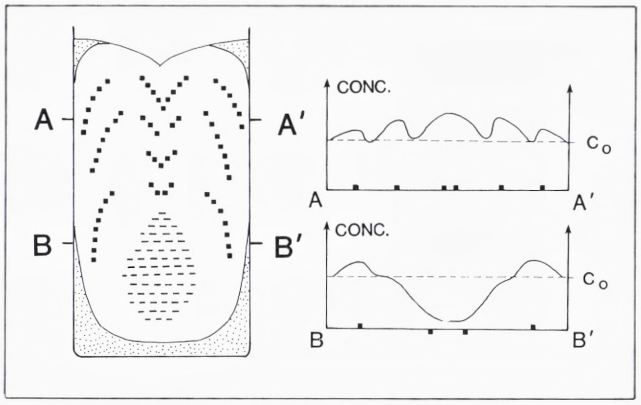

Fig. 30. Macrosegregation in typical cast ingot. Square dots mark positive segregation whereas horizontal stipple is negative segregation. Chilled products are finely dotted. Right diagrams show idealized compositional variations across two sections A-A' and B-B'. The axisymmetrical distribution is pronounced; positive segregation fluctuates in the upper portion of the ingot whereas negative segregation dominates the lower portion.

Macrosegregation is usually expressed as the relative deviation from average composition of the source melt; positive segregation corresponds to a more differentiated state while negative segregation represents a less evolved composition (Flemings, 1974). Axisymmetrical ingots often exhibit substantial segregation in the vertical as well as the horizontal direction. A typical example of macrosegregation in cast metal ingots illustrates this qualitatively: In the upper part of the ingot (cross section A-A', Fig. 30), several zones of positive segregation are separated by neutral zones and form a regular compositional variation which fluctuates through the ingot. This variation resembles the regular trend reversals in cryptic layering observed in many igneous bodies, e.g. the Stillwater Intrusion (Jackson, 1961). In a lower part of the same ingot (cross section B-B', Fig. 30), compositional variations are expressed by an outer margin of positive segregation and a core of substantial negative segregation. Geologically, this trend compares with the reverse compositional variation as found e.g. in the lardalite pluton (Petersen, 1978b). It is also comparable to the overall variation found in many anorthosite massifs, where differentiated noritic rocks form a marginal facies and more primitive anorthosites generally make up a central core (Michot & Michot, 1969; Ashwal & Seifert, 1980; Demaiffe & Hertogen, 1981).

4.2 The chain mechanism of heterogeneous nucleation

A fundamental prerequisite for solidification is the nucleation of solid phases which occurs by the condensation of sufficiently large clusters of

constituent molecules or polymers within the melt. Nucleation is classified as either heterogeneous or homogeneous, depending on whether it occurs with or without the aid of foreign substrates (Carmichael at al., 1974; Kirkpatrick, 1975; 1983). The stability of newly formed nuclei depends on their surface free energy, which is often expressed in terms of the critical size or critical radius for the nucleus at a given amount of supercooling (Shewmon, 1969). Thus, homogeneous nucleation requires a cluster of a certain size to allow subsequent growth. Below this size the nucleus will redissolve and become extinct. The tendency for heterogeneous nucleation of a particular phase can be expressed by its 'wetting' factor, which equals the cosine of the equilibrium contact angle θ (Fig. 31). The smaller this contact angle is, the smaller the volume fraction of a critical nucleus sphere will be, which produces a stable surface curvature that allows subsequent growth (Chalmers, 1964, p. 77; Shewmon, 1969, p. 160). Structural compatibility between the nucleus and the substrate surface reduces the contact angle and increases the chance for heterogeneous nucleation.

For these reasons, it is likely that all nucleation in natural magmas is heterogeneous and occurs preferentially on analogous materials (Kirkpatrick, 1975). Experimental studies of the solidification properties of natural silicate melts have strongly supported this view (Lofgren, 1983).

In a lateral cooling configuration as described above, it is probable that nucleation and growth preferentially occur on pre-existing crystals along the borders of the magma. Growth is facilitated in crystals that are in mutual contact and attached to the wall rock, as compared to freely suspended crystals, since the latent heat of crystallization can be extracted through the solid media. Any internal nucleus will eventually be overgrown and eliminated as solidification proceeds (Fig. 32). Convection in the magma interior may cause transport of early detached crystals along the magma chamber borders (Irvine, 1979). However, when transferred

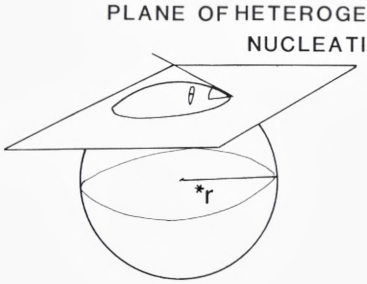

Fig. 31 The portion of an idealized, critical nucleus with radius r above the plane of heterogenous nucleation has a stable surface curvature that allows subsequent growth. The critical contact angle marks the maximum curvature of a stable surface, and thus the fraction of a critical nucleus that is necessary for heterogeneous nucleation.*

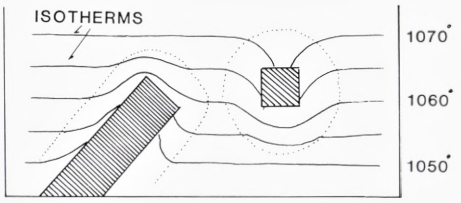

Fig. 32. Growth conditions for freely suspended versus contact-attached crystals. Heat of crystallization is build up around the freely growing crystal whereas heat can be retracted through the stem of the attached crystal. The thermal distribution thus favours growth of attached crystals over suspended individuals.

towards the hotter interior, newly formed crystals will generally dissolve, and the interior may be considered free of nuclei and fairly homogeneous within each convective unit. This applies also in the case of stratified magmas which are increasingly being accepted in the petrological litterature (e.g. Hildreth, 1979; Irvine, 1980; Huppert & Turner, 1981).

When growth of a solid phase is directed away from the heat-flow gradient, supercooling at the solidification front gradually increases because the isotherms continue to move towards the magma center at a linear rate normal to the gradient. Near the crystal interface, the isotherms are slightly deflected locally, but since the growth rate is much slower than heat-flow, this will not affect the overall increasing separation of the isotherms and the solid interface. When this separation reaches a critical value, heterogeneous nucleation will occur on the crystal face rather than continued growth, in order to achieve a higher solidification rate. This grain multiplication process is excellently illustrated by the curved dendritic pyroxenes, described in section 2; when the growth of these pyroxenes, because of the continuous curvature, becomes almost parallel to the isotherms repeated nucleation occurs on the upper surface of the dendrite (Fig. 24).

The formation of most equigranular products occurs at near-equilibrium conditions where growth anisotropy is high and solidification is interface controlled (Kirkpatrick, 1975; Gilmer, 1977). Under these conditions, the growth direction is determined by crystallographic directions of the nucleus rather than by heat flow or chemical diffusion. Low-angle branching that adjusts the growth direction at high supercooling does not occur. The maximum growth direction is therefore determined by the crystallographic orientation of the heterogeneous nucleus. The competition between maximum growth direction and maximum heat-flow direction then results in a repeated nucleation and growth process that leads to the formation of equigranular and cumulus textured pro-

ducts with a lateral solidification geometry. As the growth of a phase enriches the liquid in solute, subsequent heterogeneous nucleation of a secondary phase will likely occur on the surface of the first, where solute enrichment is highest. With the subsequent depletion of solute, the growth of the first phase is enhanced, and the process therefore leads to clustered solid aggregates.

Textural evidence showing such clustered nucleation-growth aggregates (bundle texture), is suggested to be a common, yet poorly recognized solidification structure in cumulate rocks (Campbell, 1982). The occurrence of bundle textures offers a reasonable explanation for the formation of large blocks of solidified material, e.g. along the interface of a hot, primitive magma that flows past a cooler melt, that may eventually become big enough to overcome the density-contrast, yield-strength barrier discussed by McBirney & Noyes (1979, Fig. 3), and settle through the liquid. However, it can also be the most important solidification mechanism along the cooler contacts of a magma chamber, causing crystallization to occur along a well defined interface between liquid and solid.

Preliminary experimental studies of solidification and macrosegregation of silicate melts in crucibles clearly emphasize the importance of the cluster or chain nucleation. Fig. 33 shows a two-dimensional expression of the solid-liquid interface produced with moderate supercooling. Depending on the exact cooling rate, the interface attains a regular planar or a highly irregular, indented shape. In three dimensions, the indented shape of this type of interface allows liquid to flow through the intergranular space in a manner that is analogous to interdendritic melt percolation in metallic castings (Flemings, 1974). These similarities justify the application of macrosegregation modeling in metals to silicate magmas.

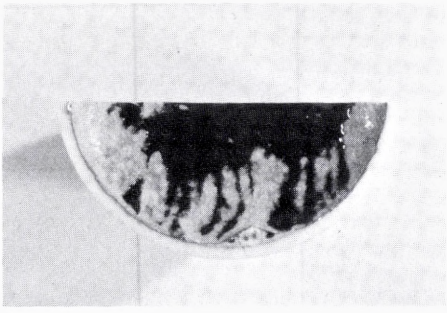

Fig. 33. Pt-plated, ceramic crucibel with 2:1 plagioclase:diopside melt cooled from 25° superheat at moderate rate. Repeated nucleation on preexisting crystals result in crystalline trains propagating towards the center. Internal nucleation is extremely rare.

4.3 Compositional variations

When a solid phase crystallizes, solute is rejected from the crystal-liquid interface. The amount of this rejection is governed by the partition coefficient at equilibrium conditions (McIntyre, 1963). At supercooled conditions, crystallization may occur isothermally, and the solid approaches the composition given by the solidus at this temperature until the continued enrichment of solute causes the melt to reach liquidus composition at C_o' (Fig. 34A). Subsequent crystallization then occurs at equilibrium conditions. When the crystallization rate is sufficiently small, the rejection of solute ultimately affects the residual liquid and gradually changes its composition. Progressive crystallization under these conditions results in a continuous enrichment of solute in the solid, as the source liquid becomes increasingly fractionated (Fig. 34B).

In the solidification of melts where the growth rate exceeds diffusion, the concentration of solute will increase near the solid-liquid interface (Fig. 34C). When a sufficiently large solute concentration has been established, one of two things may happen: diffusion of solute away from the boundary layer will keep up with the solidification rate and solidification becomes steady-state (Tiller et al., 1953; Henderson & Williams, 1977); or, the solute enrichment will reach saturation with respect to a second, near-liquidus phase (C_B in Fig. 34C).

Because the diffusion rate diminishes with the square of distance from the interface (Hoffmann, 1980), and the solidification rate at low supercooling varies linearly with time (Kirkpatrick, 1975), it is unlikely that growth attains steady-state in multicomponent systems before solute saturation occurs. Development of mono- or bimineralic products are thus generally prevented in a static melt solidification. However, when fluid flow affects a portion of the diffusive boundary layer, solute is removed at much faster rate. The conditions for a balance of input (solute production during crystallization) and output (diffusion plus removal by fluid flow) are thereby readily established, and particularly at a low absolute solute enrichment are conditions for steady-state solidification readily attained (Fig. 34D). In a closed system solute enrichment ultimately alters the source liquid and a final compositional transient of residual liquid forms which is highly fractionated (Fig. 34E). When this fraction crystallizes, the solid shows an appropriate increase in solute content.

Solute removal can be enhanced by the overlap of thermal convection in the magma interior with the diffusive boundary layer. Solute which diffuses into the convective unit cannot exceed its concentration at the

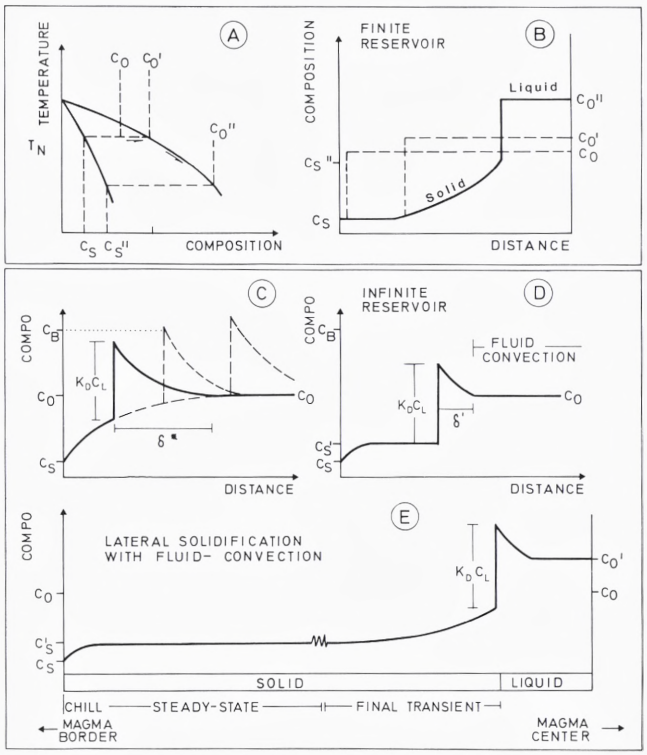

Fig. 34. Solute redistribution during plane-front solidification conditions. See text for details.

flow interface. The width of the remaining, static portion of the boundary layer δ', then determines the maximum amount of solute enrichment that develops for a given diffusion coefficient (Fig. 34D). The effect of this process can be quantified by using a different effective diffusion coefficient in the solute redistribution equations (Flemings, 1974). Thermal and rheologic properties of natural silicate magmas support the presence of fluid convection (Bartlett, 1969). Such magmas may solidify at steady-state under broadly isothermal conditions and produce nearly constant compositions after an initial transient.

A second type of fluid flow, percolating flow between growing bundles of solid phases, results in substantial mass transfer through the mushy zone of crystallization (Flemings, 1974; Mehrabian, 1984). This flow is established by a considerable volume reduction during solidification at highly irregular solidification interfaces, and is typically encountered in the dendritic solidification of metallic melts. As shown in Fig. 35, the percolating flow, however, also plays a prominent role in comparatively viscous silicate melts upon progressive solidification, and should not be overlooked.

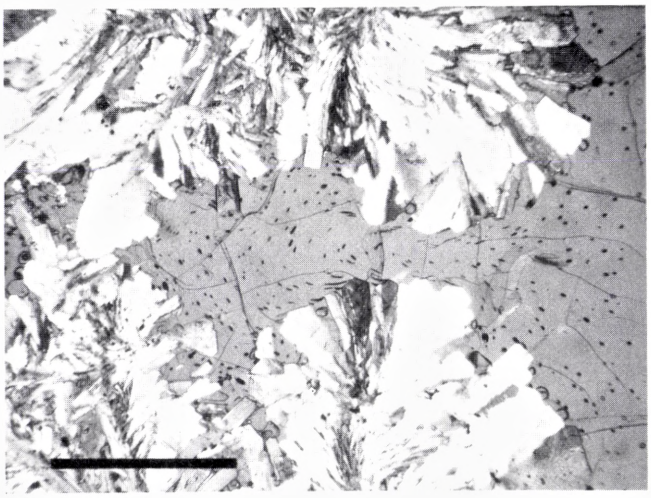

Fig. 35. Experimental charge of ternary feldspars solidified by heterogeneous nucleation and growth from the capsule walls. Deformed vapor bubbles reveal fluid flow in the intercrystalline liquid as the result of volume reduction during prograde crystallization. This indicates that significant percolation flow exists in silicate melts upon solidification. Scale bar measures 1 mm.

During steady-state solidification the solid composition is defined by the relation $C'_s = {}^{\star}k_dC_o$, where C_o is the composition of the source liquid, and ${}^{\star}k_d$ the effective partition coefficient at steady-state. The extent of steady-state crystallization depends on the differentiation of the residual liquid, and on the difference between the source liquid (C_o), and the solid product of the steady-state solidification (C'_s) (Fig. 34D). This difference is a reflection of the magnitude of the effective partition coefficient ${}^{\star}k_D$. Values of ${}^{\star}k_D$ near unity may produce substantial amounts of steady-state growth since the residual liquid is only slightly affected. In contrast, large or small ${}^{\star}k_D$-values will tend to reduce the amount of steady-state solidification since the source liquid becomes differentiated more rapidly.

The distribution of solute during lateral solidification can be modeled quantitatively and applied to polyphase systems by considering the solvent as the sum of constituent components in the solid product, and the solute as the sum of complementary components in the melt. Chemically, the characteristics of these components can be defined as a matrix of the type B = M - A, where M is the composition of the source melt; A is the composition of the solvent (= solid aggregate), and B the solute, readily calculated for various solid aggregates by e.g. petrographic mixing programmes (Wright & Doherty, 1970).

The bulk chemical modeling discussed above accounts for the overall variation of the solid product during solidification, and explains the formation of gradual changes in the initial or final transients, which may

or may not include an intervening steady-state solidification. Whether the size of the effective partition coefficient $^{\star}k_d$ is greater or less than one, the solid product may attain a prograde or a reverse, overall compositional zonation. Its application, however, is ideally restricted to a plane front solidification and simultaneous crystallization of the main constituent phases.

These conditions are readily met in eutectic crystallization where simultaneous precipitation occurs with a planar front (Flemings, 1974). The plane front is achieved because transverse diffusion and phase-spacing regulations adjust the bulk interface liquid to eutectic composition at any given growth rate, and the product solidifies at steady-state (Mollard & Flemings, 1967; Elliott, 1977). A plane front is also achieved at dendritic solidification because dendrite spacing adjusts to minimize transverse diffusion and the solute redistribution modeling becomes equivalent to that of eutectic solidification (Scherer & Uhlmann, 1975). In this case, secondary phases precipitate from the trapped interdendritic melt. Their crystallization, however, does not change the overall composition of the product. Therefore, in terms of solute redistribution, the dendritic solidification can be viewed as a special case of multicomponent solidification where one phase, because of a higher growth rate, is leading. In order to understand the more general situation, analysis of solidification geometries and kinetics of crystallization is therefore required.

4.4 The solidification geometry

Two extreme types of solidification geometries provide a useful basis for the discussion of directional chemical segregation. In one case, internal nucleation is abundant and approximately simultaneous within the entire melt fraction. Such nucleation causes spheroidal diffusion zones, enriched in residual solute, to form around each nucleus during subsequent growth (Fig. 36A-B). Because this solute enrichment occurs in an isotropic configuration, no compositional gradient exists between different portions of the melt, and the expelled inter-mineral solute cannot migrate by long-range diffusion. Solute content in the intercumulus melt therefore increases continuously with progressive crystallization and the composition of the solid phase assemblage becomes increasingly zoned and fractionated.

This type of solidification geometry, termed uniform, due to the uniform distribution of nucleation, corresponds to the traditional view on the origin of cumulate textures (Wager et al., 1960). Escape of variable

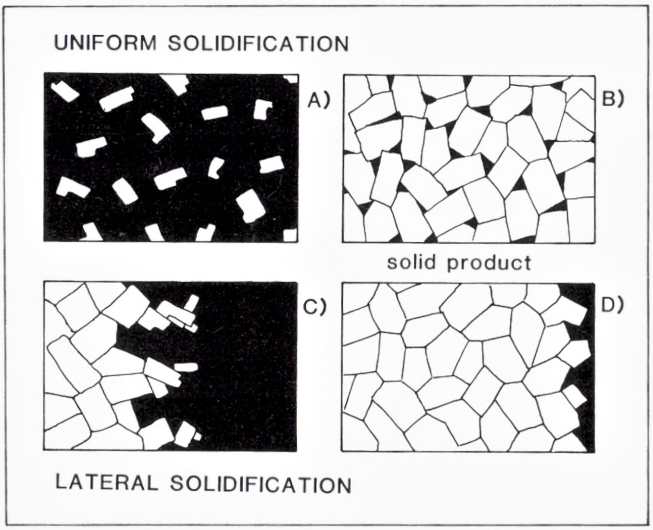

Fig. 36. Principal solidification geometries. A-B are the result of uniform nucleation and isotropic growth. C-D are formed by heterogeneous nucleation and subsequent lateral growth. The rejected solute accumulates ahead of the solidification front in D), contrary to the uniform crystallization geometry B), where solute is evenly trapped within the sample.

amounts of intercumulus liquid is required for fractionation, but the mechanisms of this segregation remain somewhat controversial. This type solidification may represent a special case, where thermal supercooling is very high, such as just after injection of the magma or when the melt is suffering from vigorous turbulent flow due to emplacement or volcanic eruption, but probably may not apply to the general solidification of resting magma chambers as often thought. Chilled margins are obvious natural examples of this type of solidification mechanism, and so are volcanic products and some porphyritic-textured, contact rocks.

In the other solidification geometry, designated here as lateral solidification, nucleation and growth project laterally from the contact zone towards the interior of the magma. This can occur by the chain nucleation and growth mechanism (Fig. 36C-D). The residual components accumulate in the boundary layer ahead of the solidification front and form a compositional gradient. This gradient creates conditions for the removal of solute by directional diffusion and fluid flow, and its ultimate accumulation in residual solidification pockets (Fig. 36D). Certain monomineralic, comb-layered rocks are obvious examples of this type of solidification (Petersen, 1985).

Either of the above solidification geometries lead to differentiation provided removal of intercumulus liquid occurs. This is often expressed by the amount of adcumulus growth (Wager et al., 1960; Wager & Brown, 1967) or by the proportion of mesostasis – pore liquid (Hender-

son, 1970). In the uniform model, the removal of interstitial solute requires an effective percolation of fluid through a densely nucleated crystal mush to produce fractionation. Since the presence of nuclei or crystalline particles increases the viscosity of the liquid substantially (Komar, 1972), this process becomes increasingly difficult. Removal of interstitial liquid by fluid flow possibly occurs during compaction by a process sometimes referred to as filter pressing, although, the capacity of this mechanism to explain enhanced adcumulus growth is limited (Bowen, 1928, p. 157; Emmons, 1940; Carmichael et al., 1974). Diffusion through the interstitial liquid is possible, but this requires the presence of an overall compositional gradient and it becomes almost prohibitively slow beyond distances on the order of the average grain size. Effective fractionation and adcumulus growth in the uniform solidification geometry is therefore difficult, and at best occurs at extremely slow solidification rates.

In contrast, the chain nucleation-growth model suggested above allows the continuous removal of excess solute during growth by diffusion into the boundary layer and by fluid flow along the solidification front. Depending upon the shape of the solidification front, planar or highly indented, this type of solidification creates a diffusive boundary layer which is more or less parallel to the isotherms, and causes compositional variations to follow a plane-front solute redistribution model. This process can therefore lead to the formation of cyclic compositional variations (type-2 layering); complementary phase layering (type-1 layering); steady-state growth of mono- or polycrystalline products, or simply gradual differentiation as was seen for the comb-layered products. The textures, however, will be those of repeated nucleation, i.e. cumulus textures instead of a columnar directional fabric. Another very important implication of the above textural considerations is that many of the planar, contact parallel structures found in igneous rocks are likely to reflect successive time interfaces during crystallization, i.e. solidification isochrons, which are parallel to the isotherms.

5. Applications of lateral solidification and macrosegregation to petrogenetic modeling

Many plutonic complexes show regular compositional variations which are readily explicable in terms of lateral solidification. In many zoned plutons, the variation, however, shows prograde differentiation from the margin towards the center, for example the Rocklin pluton (Swanson, 1978) and the Tuolumne Series (Batemann & Chappel, 1979) in Sierra Nevada, California, thus, a variation which can well be accounted for by traditional fractional crystallization. In some plutons compositional variations occur which are reverse to this trend; differentiation seems to project from the core towards the margin, and clearly present some problems with respect to traditional petrogenetic modelling.

A few examples of such 'anomalous' cases will be briefly considered here in order to illustrate advances of the macrosegregation concept over traditional petrogenetic modelling and to demonstrate the capacity of this hypothesis to account for both normal and reverse overall compositional variations as well as the formation of homogeneous or rhythmically layered solidification products.

The Hidra anorthosite-norite is a zoned intrusive body in the SW part of the Egersund anorthosite province, SW Norway (Demaiffe & Hetogen, 1981). It constitutes the youngest anorthosite body in the region and has suffered minimum post-emplacement textural modification such as granulation of feldspars and pyroxenes, contrary to most other anorthosite bodies of the province. The primary nature of this complex therefore makes its textural and compositional relations particularly significant.

The complex measures about 6 × 20 km and shows a regular concentric distribution of different rock facies. Following a narrow, fine grained and porphyritic, jotunitic border facies is a marginal, ophitic-textured norite with average grain size about 2 mm which grades into coarser norite and finally into coarse grained leuconorite and anorthosite with single feldspars measuring 5 × 15 mm and up to dm size in the core of the complex. No internal contacts between these facies have been observed.

Plagioclase occurs as cumulus feldspars with moderate, normal zonation from An_{50} to An_{45} in the central, anorthositic and leuconoritic part. The most Ca-rich feldspars from the ophitic-textured border zone, show compositions which are equivalent to the rim compositions of the inter-

ior plagioclases, about An_{45}, whereas interstitial feldspars in this zone rate about An_{35} and are additionally fairly Or-rich, about Or_{14}. These compositions accordingly suggest that the border-zone rocks are more evolved than the interior rock facies in this complex.

Ca-poor pyroxenes which constitute the dominant ferromagnesian phase in the Hidra complex, show similar relations. The interior, anorthosite hosted orthopyroxene of En_{70} forms interstitial grains, completely bounded by cumulus plagioclases. Approaching the marginal facies, both plagioclase and orthopyroxene form cumulus phases with pyroxene compositions about $En_{65}Fs_{33}Wo_2$, – thus more evolved than the interior ones. The ophitic-textured border norites show even more pronounced Fe-enrichment about $En_{57}Fs_{41}Wo_2$. Ca-rich pyroxenes are present in this zone as discrete grains, whereas elsewhere in the complex Ca-rich pyroxenes occur only as minor anhedral or interstitial grains. Biotite, apatite and interstitial K-feldspar, the latter showing a spectacular intercumulitic, symplectitic intergrowth with quartz occur exclusively in the border facies, and emphasize the more differentiated character of this part of the pluton.

In addition to the increasing mineral differentiation towards the margin, the Hidra complex also shows a significant modal increase in ferromagnesian phases from the core towards the margin, i.e. in the direction of prograde differentiation, a common feature in anorthosite massifs which led Ashwall (1982) to suggest that mafic and Fe-enriched rocks constitute residual products of anorthosite formation. Both the increasing differentiation towards the margin and the decreasing mafic content towards the center, however, are incompatible with the overall compositional variation in calc-alkaline or tholeiitic rock suites that crystallizes from the margin inwards.

The reverse compositional variation in the Hidra complex is conformable with inwards solidification assuming a decreasing cooling rate and thus increasing negative macrosegregation. Differentiated rocks formed in the initially steep thermal gradient at the margins, where removal of solute was minimum. Abundant nucleation in a thermally supercooled contact may form a chilled border facies. The ophitic textured, marginal facies of this pluton, however, are considered subsequent products of repeated nucleation and growth at subliquidus conditions, in a fairly steep thermal gradient. The rapid solidification resulted in local supersaturation and precipitation of accessory phases such as apatite and K-feldspar. Prolonged heating from the hotter interior allows solid diffusion to smoothen out the initial mineral zonations in the contact zone rocks.

Later, as the cooling rate decreases, increasing amounts of rejected solute are removed by diffusion and convection, and thus result in increasingly negative segregation. The reciprocal, residual liquid of this solidification process would become increasingly mafic in accordance with the findings of Ashwal (1982) and also accounts for the occurrence of minor, intrusive Fe-Ti ore bodies in the district.

A number of small intrusive, alkali-rich gabbroic stocks, less than 400 m wide, which additionally occur in the anorthosite province of south Norway, reveal interesting analogies in composition and textures with the ophitic-textured border facies of the Hidra massif. In contrast to the compositionally zoned anorthosite-norite complex, these minor gabbro plugs are exceedingly homogeneous and display no variation from the border towards the center. Instead, a remarkable zonation is given by the constituent minerals which support the textural relations in suggesting an enhanced, in situ fractionation.

In one of these stocks, the Lyngdal hyperite, plagioclases are lath shaped about 1 × 4 mm and display normal zonation from about An_{45} to antiperthitic margins about An_{35}. Myrmekitic fringes on the antiperthitic margins project into interstitial orthoclase and quartz. This textural sequence is comformable with a closed-system fractionation with progressive build up of residual components in the trapped interstitial liquid. The formation of myrmekitic fringes may actually represent coordinated growth of a cotectic plagioclase-quartz pair which is succeeded by residual quartz or K-feldspar as indicated by the textural relations. Ca-poor pyroxenes are the predominant ferromagnesian minerals in the hyperite and span a fairly narrow range from about En_{63} to En_{59}. Apatite is abundantly present and forms stubby euhedral grains.

Despite the immediate differences in texture and compositional variation between these two plutons, remarkable similarities exist. The range of feldspar and pyroxene compositions in the anorthosite complex is almost identical to that of the zoned minerals of the hyperite. The latter variation, however, projects from the center of single crystals into the interstitial space, while the former shows the same overall variation from the core of the complex to the margin, although, as mentioned, opposite to the expected trend of differentiation.

The contrasting textural evolution of these two plutons is summarized in Fig. 37. In a closed system, such as the marginal facies of the Hidra complex or the Lyngdal hyperite intrusion, early Ca-rich plagioclase becomes progressively more Na-rich when poikilitic pyroxene joins the assemblage (Fig. 37,1-2). Subsequently, plagioclases with antiperthitic

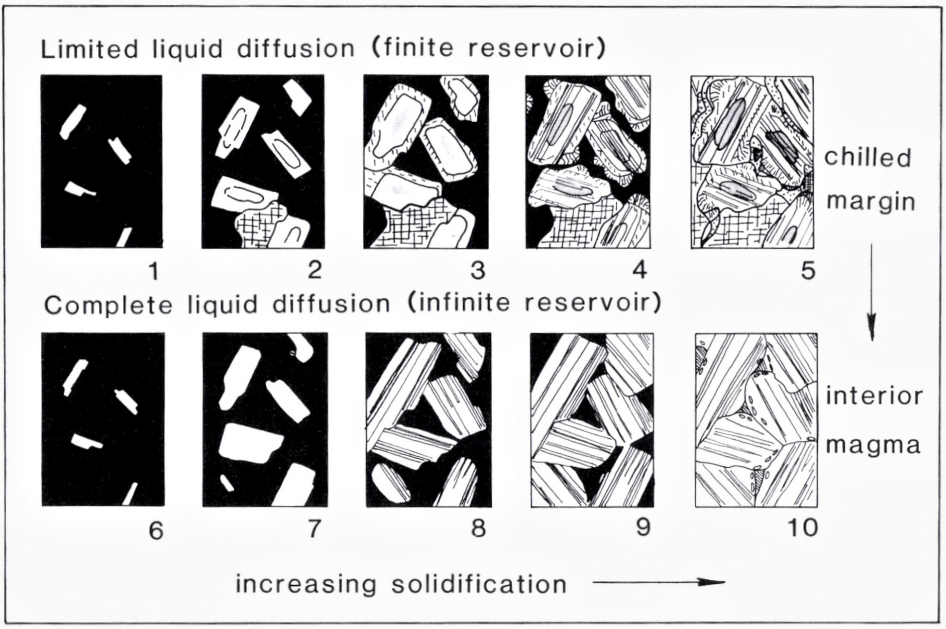

Fig. 37. Contrasting solid products as formed by different solidification conditions. 1-5 show the progressive fractionation in a uniform solidification geometry with no liquid diffusion. The solid product (5) equals the composition of the initial liquid (1). In 6-10, the initial liquid (6) is similar to that above. Removal of excess solute due to liquid diffusion and/or lateral solidification geometry, allows continued precipitation of the initial phase assemblage (7-8).

exsolution lamellae develop (3), which later grade into myrmekitic fringes (4) and ultimately into interstitial quartz and K-feldspar (5), which mark the closing compositions. Apatite may additionally form in local, supersaturated boundary liquids. This sequence completely mimics the textural variation observed in the Lyngdal hyperite.

The other extreme, illutrated by Fig. 37, 6-10, forms when solute is removed from the intercrystalline liquid. Depending on the solidification geometry this process can allow perfect adcumulus growth and continuous precipitation of the initial, high-temperature phases as long as the source liquid composition and the solidification conditions remain constant. A complete gradation from case 1-5 at the margin of the intrusive body to case 6-10 in the core can be expected in the course of crystallization and progressive cooling. In case of the anorthosite body, prolonged cooling at subliquidus temperatures may gradually eliminate initial mineral zonations in the marginal facies. Identical geochemical properties of the Lyngdal hyperite and the marginal facies of the Hidra

complex, including trace element data (Petersen, in prep.), show that the former may represent an appropriate parent magma for anorthosite.

In a similar case of competitive nucleation and growth, oscillating chemical variations in the boundary layer can relate to the formation of complementary phase layering. Two principal types of layering found in the predominantly homogeneous larvikite intrusions of the southern Oslo region emphasize this point. One type is graded, compositional phase layering, with sharp lower contacts, that is equivalent to Skaergaard type layering except for its nearly vertical orientation, which makes an origin by gravitative crystal settling difficult. The other type, which is slightly more common, is characterized by faint layering caused by the cyclic appearance of intercumulus, poikilitic pyroxenes. This variety, which is even more difficult to relate to a crystal settling origin, is explicable by the periodic nucleation of faster growing pyroxenes along isotherms that follow a nearly planar front. These examples show that the composition of the solid product depends not entirely on the compositional gradient in the boundary layer, but also on the kinetics of the crystallization, such as the relative nucleation and growth rates.

One of the important features of the repeated nucleation and lateral solidification suggested here, is that solidification occurs along isotherms, which are broadly parallel to the contacts. This will produce a largely concentric solidification pattern. Accordingly, any changes in the crystallization conditions, such as the formation of rhythmic or cryptic layering, are to be recorded along these concentric interfaces. Differences in the thermal gradients (cooling-rate), on the other hand, may cause the phase assemblages to change along the solidification front.

A possible example of this is shown in the Farsund charnockite, SW Norway which was injected adjacent to major anorthosite massifs of SW Rogaland, that produced a substantial thermal gradient in the country rocks as indicated by pronounced metamorphic aureoles. The concentric pattern of e.g. the FeO content in the charnockite (Fig. 38) is conformable with a solidification along isotherms from the margin inwards. The phase assemblages and compositional properties of the constituent minerals, however, vary laterally across the pluton and exhibit more primitive compositions in the southeastern, more rapidly cooled part, and higher temperature assemblages like fayalite instead of orthopyroxene in the northwest (Petersen, in prep.).

The interference between isotherms and cooling rate changes may particularly affect the composition of the solid products in a flat sheet of magma, where cooling rate at the extremities will be much higher than

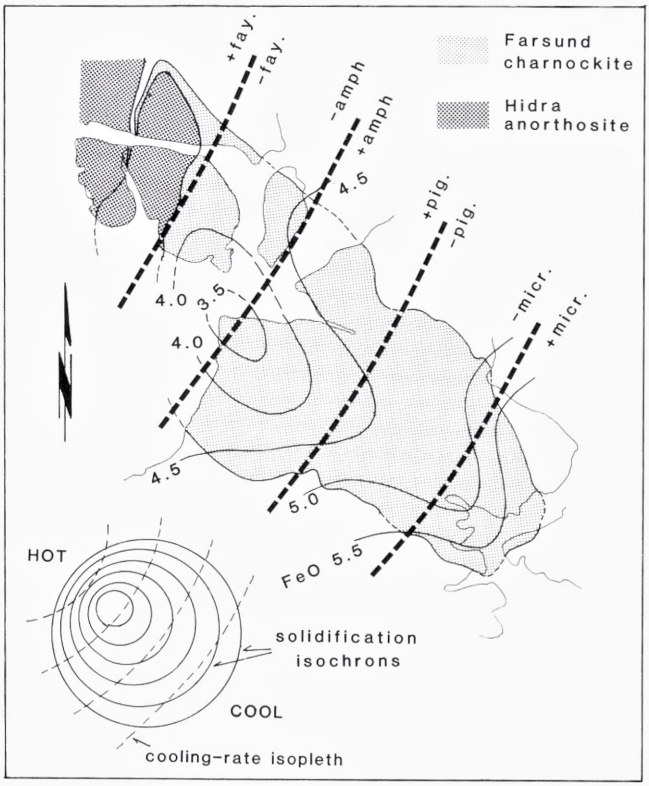

Fig. 38. Concentric patterns of isotherms and solidification fronts can be reflected by cryptic compositional layering such as the FeO-content in the Farsund charnockite. Cooling rate isopleths which influence the phase assemblages, however, can vary across the pluton according to a regional thermal gradient.

the central portion. Fig. 39 shows a cooling-rate isopleth of such a magma type following the data of Jaeger (1968). In the flat sheet, the isotherms will follow the boundaries, and the solidification interfaces therefore become practically horizontal. A pronounced, lateral, compositional variation along the solidification front can therefore develop due to changing cooling-rate and different diffusion efficiency; the rapidly cooled extremities will appear more differentiated because of higher amounts of trapped residual liquid here, whereas progressively slower cooled parts will appear less differentiated because of the increasing efficiency of solute removal. Such a spectacular, discordant relationship between rhythmic and cryptic layering was recently discovered in the layered Fongen gabbro, central Norway (Wilson & Larsen, 1982).

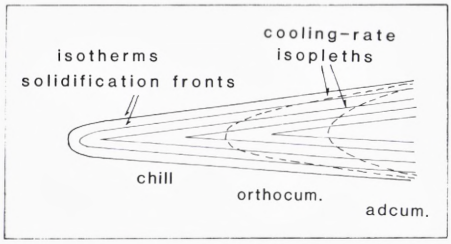

Fig. 39. In flat magma sheets, cooling rate at the extremities is high and allows little liquid diffusion. In the more interior portions of the magma, solute removal becomes increasingly important and thus implies changing phase assemblages which essentially follow the cooling rate isopleths. Solidification interfaces, on the other hand, are largely parallel to the contacts and thus possibly cross-cut the cooling rate isopleths, producing discordant relations between growth structures and phase assemblages.

6. Summary and conclusions

Directional solidification textures reveal important information about the conditions of crystallization which is not recognizable in isotropically textured products. Because the crystallization occurs sequentially from the contacts and inwards, analysis of thermal and compositional variations during directional solidification can be related to distance and time: systematic changes in crystal shapes are the result of different growth mechanisms which in turn reflect variable supercooling during crystallization; different mineral assemblages and their compositions reflect changing thermal conditions during the solidification; and finally, overall compositional variations permit evaluation of some kinetic properties of the constituent phases and the dynamic conditions in the source melt.

In the lardalite contact zones, crystal shapes near the margins are fan dendritic, the result of high thermal supercooling presumably following the emplacement of a hot magma into a cooler environment. Subsequent columnar growth with anisotropic, cellular textures imply growth by crystallographic control. At least one facet is required for the consistent orientation in the compact solid products and indicates that supercooling was above the roughening temperature of one crystallographic plane. Two facet planes subsequently promote the formation of columnar rod-shaped crystals, with growth restricted in two lateral directions. Unconstrained growth in the third dimension is directed parallel to heat flow. Consistent orientation of the 010 plane normal to the maximum growth direction in the columnar feldspars show that this face was the last to develop faceted growth, in accordance with its loose atomic packing and thus high roughening temperature. When growth is controlled by three

facet planes, the main elongation is controlled by crystallographic properties and deflected away from the direction of maximum heat flow; at this stage, the crystals start growing at an angle to the isotherms.

Growth in supercooled conditions results, in addition to low angle branching, in the formation of curved lattice planes which are readily recognised from curved polysynthetic twin planes and undulous extinction sweeping across individual subgrains upon rotation of the sample in plane polarized light. Apparently, the higher the supercooling during solidification is, the higher lattice curvature is achieved. The intersection of such curved lattice planes with growth facets, results in curved crystal shapes, formed in a completely static environment. Because of this curvature, the maximum growth is gradually directed away from the heat flow. When the growth of a curved dendrite becomes almost parallel to the isotherms, the isotherms move away from the solidification front, and repeated heterogenous nucleation occurs on top of the curved dendrite in order to readjust growth towards the heat flow. The dendritic crystallization thereby continuously adjust the solidification geometry to a maximum rate. Similarly, is the spacing of the dendrites continuously adjusted to optimum growth conditions. This happens because transverse diffusion between neighbouring dendrites readjusts the spacing to the actual growth conditions by eliminating excess dendrites, when the diffusion range is increasing, or allows subsequent bifurcation when the diffusion range is decreasing.

Directional growth occurs when a zone of constitutional supercooling is developed ahead of the solidification front. The changing crystal shapes in the lardalite contact zones show that thermal supercooling decreases continuously inwards whereas constitutional supercooling initially rises to a maximum and then decreases gradually until its ultimate extinction. When constitutional supercooling is eliminated, the crystallization produces equigranular textures. The presence of dendrites in some porphyritic textured zones, however, shows that the conditions for constitutional supercooling is eliminated sequentially for different phases, and thus that the porphyritic textures are formed by directional solidification despite the lack of textural evidence. This fact justifies the interpretation of equigranular and cumulus textured products in terms of lateral, directional solidification with repeated, sequential nucleation.

Compositional variations in the directionally solidified contact zones demonstrate that large compositional gradients are produced in a static boundary layer. The build up of solute and subsequent precipitation of complementary phases may lead to rhythmic layering comparable to

Skaergaard type layering. Also, remarkable examples of steady-state crystallization, which include compact, monomineralic layers, show that solute removal from the boundary layer occasionally balances the production at the solid-liquid interface. This type diffusion-controlled solidification occurs when the solid product approaches the composition of the liquid or when excess solute is removed by fluid flow, such as by convection near the crystallization front. The solute redistribution in these cases can be approximated by plane-front solidification models derived from binary systems by considering solvent as the bulk composition of the solid and solute as the sum of residual components.

In entirely equigranular products the direction of crystallization is not directly observable. The similarity of the contact zones with macrostructures of typical cast metal ingots, which include a chilled border zone, a columnar textured, marginal facies and an inner equigranular zone (Chalmers, 1964; Bolling, 1969; Flemings, 1974), suggests that the formation of equigranular textured pluton interiors is a product of directional solidification, and that the directional solidification of single phases in comb-textured contact zones is succeeded by repeated, heterogeneous nucleation of multifaceted crystals when constitutional supercooling is eliminated. In these conditions can compositional variations be ascribed to macrosegregation and dynamic solidification processes.

The concept of macrosegregation accounts for the overall compositional variation produced during solidification. Macrosegregation occurs primarily from fluid flow in the crystallization zone, and includes both laminar, convective flow along a planar solidification front and percolation flow in a mushy crystallization zone. This fluid flow serves to remove solute from the crystallization front. The flow interface, however, is invariably separated from the solid interface by a boundary layer of static liquid, in which transfer of solute occurs only by diffusion. The width of this static boundary layer controls the solute enrichment at the solid liquid interface, since the concentration of solute at the flow interface cannot exceed that of the flow unit; a wide boundary layer allows high solute concentration gradients whereas a narrow layer promotes minimum solute enrichment.

Crystallization with minimum supercooling in a magma at rest occurs mainly by heterogeneous nucleation along the cooler margins. Removal of heat of crystallization through solid media favours growth of crystals which are interconnected and attached to the wall rock relative to crystals in liquid suspension. The main solidification can therefore occur by a

chain nucleation and growth mechanism that creates a well defined solid-liquid interface, presumably subparallel to the isotherms.

In such a lateral solidification geometry, rejected solute accumulates ahead of the solidification front and is potentially removed by diffusion and fluid flow. Steady-state solidification may occur when solute enrichment in the boundary layer remains constant. This happens when a balance between solute build up at the solid interface and solute removal from the boundary layer at the flow interface is established. Quantitative modeling of the solute redistribution is possible when the solidification conditions are known. These conditions require knowledge of the diffusion coefficients, the solidification rate and width of the static boundary layer. Effective partition coefficients about unity readily form steady-state because the solute enrichment is minimum. High or low partition coefficients on the other hand require enhanced solute removal, such as by convective flow near the solid interface, for steady-state.

Extreme adcumulus growth can be treated as steady-state, monophase precipitation with repeated nucleation; excess solute which would otherwise result in precipitation of secondary phases is continuously removed from the crystallization front by fluid flow along a narrow static boundary layer. If the removal of solute is limited, e.g. in a wide static boundary layer, periodic precipitation of secondary liquidus phases may lead to the formation of rhythmic compositional layering.

Macrosegregation is expressed by the compositional difference between the solid product and the source liquid and referred to as positive or negative. Initially large thermal supercooling near the contacts results in abundant nucleation and minimum segregation (chilled products). Later, when the cooling rate decreases, progressive removal of solute from the crystallization zone results in an increasingly negative segregation. Positive segregation ($\sim$ differentiation) cannot preceed negative segregation in a closed system. Magmas which show progressive, negative segregation towards the center (increasing adcumulus growth or reverse compositional zonation), accordingly must include a complementary liquid in order to account for the positive segregation in their petrogenesis.

Decreasing cooling rate towards the interior of a solidifying magma increases the time available for diffusion. A transition from predominantly orthocumulus growth (non-segregated) to predominantly adcumulus growth is therefore to be expected with continuous cooling. The result is a progressive, negative segregation. Because the solute

accumulation ultimately effects the source liquid, a final positive segregation can develop. In continuous castings with a planar solidification front, this positive segregation is usually experienced in restricted parts of the upper portion of the ingot, whereas the major, generally lower part suffers pronounced negative segregation.

Convection along a planar solidification front allows substantial amounts of the source magma to pass the crystallization zone and thus the precipitation of disproportionate amounts of selected phases, depending on their nucleation and growth characteristics. Because of the static boundary layer, the solute accumulation may attain any concentration level between that of the source liquid and the maximum enrichment at the solid interface; the solid phase assemblage thus 'sees' a source liquid whose composition depends only on the width of the boundary layer. Clearly, in such cases, the modelling of fractionation paths with the use of equilibrium phase relations has little significance for the evolution of the true source magma.

Lateral solidification with a planar or pseudoplanar front tends to follow the isotherms, which in turn reflect the cooling surface and the position of the solid-liquid interface. The formation of planar solidification structures such as rhythmic layering and textural lamination may therefore follow these planes and so define crystallization isochrons. Differentiation in the sense of macrosegregation, however, essentially reflects the dynamics of the solidification process, i.e. the cooling and fluid flow rates and the time available for solidification. Important differences in composition may therefore develop laterally if thermal gradients change along the solidification front; orthocumulus growth will predominate in steep thermal gradients whereas adcumulus growth controls more gentle crystallization conditions.

The discussion of compositional variations in magmas as a result of dynamic crystallization processes and macrosegregation is new to petrological thinking. In the previous decades main emphasis of petrogenetic modeling in plutonic rocks was placed on equilibrium phase relations, and differentiation based on various derivations of surface or total equilibrium crystallization models.

Fluid dynamical processes as a source of magma differentiation have been increasingly recognized in the literature, and are likely to contribute to the overall differentiation. Such processes include transport of crystals through the liquid by gravity induced convection (Irvine, 1979; Rice, 1981), double-diffusive convection (Turner, 1973, 1980; Turner & Gustavson, 1978; Chen & Turner, 1980; McBirney & Noyes, 1979; Huppert

& Turner, 1981), Soret or Dufour separation (Walker et al., 1981) and/or liquid imiscibility (Philpotts, 1976; Roedder, 1979). As the above processes essentially derive from liquid-liquid interactions they represent additional cases of magma evolution which are beyond the scope of this paper.

The solid-liquid interface, however, constitutes the most important transformation boundary which relates directly to the composition of the solid products. The present discussion is aimed at compositional and textural variations in the solid products which derive from processes at the solid-liquid interface, rather than on changes in the source liquids. This does not exclude important effects of the latter process, but the effects of such processes are considered secondary to those developed at the solid-liquid interface.

Rigorous quantitative approaches have deliberately been excluded from the text because, although quantitative solutions to many problems related to macrosegregation and crystallization kinetics are established for metallic systems, little experimental information is yet available for multicomponent silicate systems. The discussion, however, shows that a variety of important petrological phenomena, which include features that occasionally violate equilibrium phase relations, can be related to a single, dynamic solidification model.

ACKNOWLEDGEMENTS. *I am grateful to Dr. Gary Lofgren, Experimental Petrology Branch at the Solar System Exploration Division, NASA, Johnson Space Center, Houston, for providing excellent research facilities during the tenure of a visiting fellowship. I wish to thank Dr. D. Gust, Lunar and Planetary Institute, and Dr. G. E. Lofgren, NASA-JSC for critically reading the manuscript and providing valuable suggestions. Dr. J. R. Wilson, Aarhus Univ., kindly commented upon early parts of the paper. Microprobe analyses at the Univ. of Oslo and NASA-SSED are also much appreciated.*

References

Allègre, C. J., Provost, A., & Jaupart, C., 1981: Oscillatory zoning: a pathological case of crystal growth. *Nature 294,* 223-228.

Ashwal, L. D., 1982: Mineralogy of mafic and Fe-Ti oxide-rich differentiates of the Marcy anorthosite massif, Adirondacks, N.Y. *Am. Miner 67,* 14-27.

Ashwal, L. D. & Seifert, K. E., 1980: Rare-earth-element geochemistry of anorthosites and related rocks from the Adirondacks. *Bull. Geol. Soc. Am. 91,* 659-684.

Baragar, W. R. A., 1960: Petrology of basaltic rocks in part of the Labrador Trough. *Bull. Geol. Soc. Am. 71,* 1589-1644.

Bartlett, R. R., 1969: Magma convection, temperature distribution and differentiation. *Am. Jour. Sci. 269.* 1067-1982.

Batemann, P. C. & Chappel, B. W., 1979: Crystallization, fractionation and solidification of the Tuolumne intrusive series, Yosemite National Park, Calif. *Bull. Geol. Soc. Am. 90,* 465-482.

Bhattacharji, S., & Smith, C. H., 1964: Flowage differentiation. *Science 145,* 150-153.

Bolling, G. F., 1969: Manipulation of structure and properties. In: *Solidification.* Amer. Soc. Metals, Metals Park Ohio, 341-385.

Bowen, N. L., 1928: *Evolution of the Igneous Rocks.* Princeton Univ. Press.

Brown, G. M., 1956: The layered ultrabasic rocks of Rhum, Inner Hebrides. *Phil. Trans. Roy. Soc. Lond. Ser-B,* 1-53.

Bryan, W. B., 1972: Morphology of quench crystals in submarine basalts. *J. Geophys. Res. 77,* 5812-5219.

Buerger, M. J., 1934: The lineage structure of crystals. *Z. Kristallogr. Miner. 89,* 195-220.

Campbell, I. H., 1978: Some problems with the cumulus theory. *Lithos 11,* 311-323.

Campbell, I. H., 1982: Layered intrusions: a mini review. In: D. Walker & I. S. McCallum (eds.) *Magmatic Processes of Early Planetary Crusts: Magma Oceans and Stratiform Layered Intrusions.* Lunar & Planet. Inst. T.Publ. 8201, 62-65.

Carmichael, I. S. E., Turner, F. J., & Verhoogen, J., 1974: *Igneous Petrology.* McGrawhill.

Chalmers, B., 1964: *Principles of Solidification.* J. Wiley & Sons.

Chen, F. F. & Turner, J. S., 1980: Crystallization in a double-diffusive system. *J. Geophys. Res. 85, 5B,* 2573-2593.

Demaiffe, D., & Hertogen, J., 1981: Rare earth element geochemistry and strontium isotope composition of a massif-type anorthositic-charnockitic body: The Hidra Massif. *Geochim. Cosmochim. Acta 45,* 1545-1561.

Donaldson, G. H., 1976: An experimental investigation of olivine morphology. *Contr. Min. & Petrol. 57.* 187-213.

Donaldson, C. H., 1977: Laboratory duplication of comb layering in the Rhum pluton. *Min. Mag. 41,* 323-336.

Donaldson, C. H., 1983: Spinifex-textured komatiites: a review of textures, composition and layering. In: N. T. Arndt & E. G. Nisbet (eds.) *Komatiites,* 213-243.

Donaldson, C. H., Usselman, T. M., William, R. J., & Lofgren, G. E., 1975: Experimental modeling of the cooling histories of Apollo 12 olivine basalts. *Proc. 6th Lunar Sci. Conf.,* 843-879.

Donaldson, C. H., Drever, H. I., & Johnston, R., 1977: Supercooling on the lunar

surface: a review of analogue information. *Phil. Trans. Roy. Soc. Lond. Ser.-A 285,* 207-217.

Dowty, E., 1980: Crystal growth and nucleation theory and the numerical simulation of igneous crystallization. In: R. B. Hargraves (ed.) *Physics of Magmatic Processes.* Princeton Univ. Press, 419-486.

Drever, H. J. & Johnston, R., 1972: Metastable growth patterns in some terrestrial and Lunar rocks. *Meteoritics 7,* 327-340.

Elliott, R., 1977: Eutectic solidification. *Int. Metals. Rev. 219,* 161-186.

Emmons, R. C. 1940: The contribution of differential pressures to magmatic differentiation. *Am. Jour. Sci. 238,* 1-21.

Fenn, P. M., 1977: The nucleation and growth of alkali feldspars from hydrous melts. *Can. Miner., 15,* 135-161.

Flemings, M. C., 1974: *Solidification Processing.* McGraw-Hill.

Gibb, F. G. F., 1974: Supercooling and the crystallization of plagioclase from a basaltic magma. *Min. Mag. 39,* 641-653.

Gilmer, G. H., 1977: Computer simulation of crystal growth. *J. Cryst. Growth. 42,* 3-10.

Grove, T. L., 1978: Cooling histories of Luna 24 very low Ti (VLT) ferrobasalts: an experimental study. *Proc. 9th Lunar Sci. Conf.* 565-584.

Grove, T. L., & Walker, D., 1977: Cooling histories of Apollo 15 quartz normative basalts. *Proc. 8th Lunar Sci. Conf.* 1501-1520.

Grove, T. L. & Beaty, D. W., 1980: Classification, experimental petrology and possible volcanic histories of the Apollo 11 high-K basalts. *Proc. 11th Lunar Sci. Conf.* 149-177.

Harker, A., 1909: *The Natural History of Igneous Rocks.* Macmillan.

Hartman, P., 1973: Structure and morphology. In: P. Hartman (ed) *Crystal Growth: An Introduction.* North Holland, 367-402.

Hartman, P., 1982: Crystal faces: structure and growth. *Geol. Mijnbouw, 61,* 313-320.

Henderson, P., 1970: The significance of the mesostasis of basic layered igneous rocks. *J. Petrology 11,* 463-473.

Henderson, P, & William, C. T., 1977: Variations in trace element partitioning as function of crystal growth rate. In: L. H. Ahrens (ed.) *Origin and Distribution of the Elements 2. Symp.,* 191-198.

Hess, H. H., 1938: Primary banding in norite and gabbro. *Trans. Am. Geophys. Union 19th Ann. Mtg.,* 264-268.

Hildreth, W., 1979: The Bishop Tuff: Evidence for the origin of compositional zonation in silicic magma chambers. *Geol. Soc. Am. Sp. Pap. 180,* 43-75.

Hofmann, A. W., 1980: Diffusion in natural silicate melts: a critical review. In: R. B. Hargraves (ed.) *Physics of Magmatic Processes,* Princeton Univ. Press, 385-418.

Howarth, J. A., & Mondolfo, L. F., 1962: Dendritic growth. *Acta Metall. 10,* 1037-1042.

Hunt, J. D., & Hurle, T. J., 1968: The structures of faceted/nonfaceted eutectics. *Trans. Metall. Soc. AIME 242,* 1043-1047.

Huppert, H. E., & Turner, J. S., 1981: Double diffusive convection. *J. Fluid Mech. 106,* 299-329.

Irvine, T. N., 1979: Rocks whose composition is determined by crystal accumulation and sorting. In: H. S. Yoder (ed.) *The Evolution of the Igneous Rocks. Fiftieth Anniversary Perspectives.* Princeton Univ. Press, 245-306.

Irvine, T. N., 1980: Magmatic infiltration metasomatism, double-diffusive fractional crystallization and adcumulus growth in the Muskox intrusion and other layered intrusions. In: R. B. Hargraves (ed.) *Physics of Magmatic Processes,* Princeton Univ. Press, 325-384.

Jackson, E. D., 1961: Primary textures and mineral associations in the ultramafic zone of the Stillwater Complex, Montana. *Prof. Pap. U.S. Geol. Surv 358.*

Jackson, K. A., 1958: Mechanism of growth. In: R. H. Doremus, B. W. Roberts & P. Turnbull (eds.) *Growth and Perfection of Crystals.* J. Wiley & Sons, 319-359.

Jackson, K. A., 1972: Defect formation, microsegregation and crystallization morphology. In: *Solidification.* Amer. Soc. Metals., Metals Park Ohio, 121-154.

Jackson, K. A & Hunt, J. D., 1966: Lamellar and rod eutectic growth. *Trans. Metall. Soc. AIME 236,* 1129-1142.

Jaeger, J. C., 1968: Cooling and solidification of igneous rocks. In: H. H. Hess (ed.) *Basalts. Vol. 2;* Wiley, 503-536.

Jahns, R. H. & Tuttle, O. F., 1963: Layered pegmatite-aplite intrusives. *Min. Soc. Am. Spec. Pap. 1,* 78-92.

Keith, H. D. & Padden, F. J., 1963: A phenomenological theory of spherulitic crystallization. *J. Appl. Phys. 34,* 2409-2421.

Kirkpatrick, R. J., 1975: Crystal growth from the melt: a review. *Am. Miner. 60,* 798-814.

Kirkpatrick, R. J., 1981: Kinetics of crystallization of igneous rocks. In: A. C. Lasaga & R. J. Kirkpatrick (eds.) Kinetics of geochemical processes. *Min. Soc. Am. Rev. in Min. 8,* 321-398.

Kirkpatrick, R. J., 1983: Theory of nucleation in silicate melts. *Am. Miner. 68,* 66-77.

Komar, P. D., 1972: Mechanical interaction of phenocrysts and flow differentiation of igneous dikes and sills. *Bull. Geol. Soc. Am. 83,* 973-988.

Lofgren, G. E., 1974a: An experimental study of plagioclase crystal morphology: isothermal crystallization. *Am. Jour. Sci. 274,* 243-273.

Lofgren, G. E., 1974b: Temperature induced crystallization in synthetic plagioclase feldspars. In: W. S. Mackenzie & J. Zussmann (eds.): *The Feldspars.* Machester Univ. Press, 362-375.

Lofgren, G. E., 1977: Dynamic crystallization experiments bearing on the origin of textures in impact generated liquids. *Proc. 8th Lunar Sci. Conf.* 2079-2095.

Lofgren, G. E., 1980: Experimental studies on the dynamic crystallization of silicate melts. In: R. B. Hargraves (ed.) *Physics of Magmatic Processes.* Princeton Univ. Press, 487-552.

Lofgren, G. E., 1983: Effect of heterogeneous nucleation on basaltic textures: a dynamic crystallization study. *J. Petrology 24,* 229-255.

Lofgren, G. E., Donaldson, G. H., Williams, R. J., Mullins, O. & Usselman, T. M., 1974: Experimentally reproduced textures and mineral chemistry of Apollo 15 Qz-normative basalts. *Proc. 5th Lunar Sci. Conf.,* 549-567.

Lofgren, G. E. & Donaldson, G. H., 1975: Curved, branching crystals and differentiation in comb-layered rocks. *Contr. Miner. Petrol. 49,* 309-319.

Lofgren, G. E. & Gooley, R., 1977: Simultaneous crystallization of feldspar intergrowth from the melt. *Am. Miner. 62,* 217-228.

McBirney, A. R., & Noyes, R. M., 1979: Crystallization and layering of the Skaergaard Intrusion. *J. Petrology, 20,* 487-554.

McIntire, W. L., 1963: Trace element partition coefficients – a review of theory and application to geology. *Geochim. Cosmochim. Acta 27,* 1209-1264.

Mehrabian, R., 1984: A review of our present understanding of macrosegregation in ingots (abs.) In: *Fundamentals of Alloy Solidification Applied to Industrial Processes.* NASA Conf. Publ. 2337, 169-185.

Michot, J & Michot, P., 1969: The problem of anorthosites: The south Rogaland igneous complex, SW Norway. In: Y. W. Isachsen (ed.) *Origin of Anorthosites and Related Rocks.* N. Y. State Mus. Serv. Mem. 18, 399-410.

Miller, C. E., 1977: Faceting transition in melt-grown crystals. *J. Cryst. Growth 42,* 357-363.

Mollard, F. R., & Flemings, M. C., 1967: Growth of composites from the melt – part 1. *Trans. Metall. Soc. AIME 239,* 1526-1533.

Moore, J. G., & Lockwood, J. P., 1973: Origin of comb layering and orbicular structure. Sierra Nevada Batholith, California *Bull. Geol. Soc. Am. 84,* 1-20.

Morris, L. R., & Winegaard, W. C., 1969: The cell to dendrite transition. *J. Cryst. Growth 6,* 61-66.

Morse, S. A., 1970: Alkali feldspars with water at 5 kbar pressure, *J. Petrology 11,* 211-253.

Morse, S. A., 1979: Influence of augite on plagioclase fractionation. *J. Geol. 87,* 202-208.

Morse, S. A., 1980: *Basalts and Phase diagrams.* Springer-Verlag.

Nesbitt, R. W., 1971: Skeletal crystal forms in the ultramafic rocks of the Yilgarn Block, Western Australia: evidence for an Archaean ultramafic liquid. *Geol. Soc. Aust. Sp. Publ. 3,* 331-348.

Neumann, E.-R., 1976: Compositional relations among pyroxenes, amphiboles and other mafic phases in the Oslo region plutonic rocks. *Lithos 9,* 85-109.

Oftedahl, C., 1948: Studies on the igneous rocks complex of the Oslo region. IX. The feldspars. *Skr. Norske. Vid.-Akad. Oslo I. Mat.-naturv. Kl. 3.*

Petersen, J. S., 1978a: Structure of the larvikite-lardalite complex, Oslo region, Norway, and its evolution. *Geol. Rundsch. 67,* 330-342.

Petersen, J. S., 1978b: Southern part of the Oslo-rift. In: J. A. Dons & B. T. Larsen (eds.) The Oslo Paleorift. *Nor. Geol. Unders. 337,* 171-182.

Petersen, J. S., 1985: Columnar-dendritic feldspars in the lardalite intrusion, Oslo region, Norway: 1 Implications for unilateral solidification of a stagnant boundary layer. *J. Petrology 26,* 223-252.

Philpotts, A. R., 1976: Silicate liquid immicibility: Its probable extent and petrogenetic significance. *Am. Jour. Sci. 276,* 1147-1177.

Platten, I. M., & Watterson, J. S., 1969: Oriented crystal growth in some tertiary dykes. *Nature 223,* 286-287.

Poldervaart, A. & Taubeneck, W. H., 1959: Willow-Lake type layered intrusions. *Bull. Geol. Soc. Am. 70,* 1393-1398.

Rice, A., 1981: Convective fractionation: A mechanism to provide cryptic zoning (macrosegregation), layering, crescumulates, banded tuffs and explosive volcanism in igneous processes. *Jour. Geophys. Res. 86; B1,* 405-417.

Rinne, F., 1926: Thermotaxie als problem der orientierten kristallisation. *Zeitsch. Krist. 64,* 71-75.

Roedder, E., 1979: Silicate liquid immicibility in magmas. In: H. S. Yoder (ed.) *The Evolution of the Igneous Rocks. Fiftieth anniversary prespective.* Princeton Univ. Press, 15-57.

Rohatgi, P. K. & Adams, C. M. Jr., 1967: Effect of freezing rates on dendritic solidification of ice from aqueous solutions. *Trans. Metall. Soc. AIME 239,* 1729-1736.

Rutter, J. W. & Chalmers, B., 1953: A prismatic substructure formed during solidification of metals. *Can. J. Phys. 31,* 15-39.

Scherer, G. W. & Uhlmann, D. R., 1975: Diffusion-controlled growth of dendrite arrays. *J. Cryst. Growth 30,* 304-310.

Schiffmann, P. & Lofgren, G. E., 1982: Dynamic crystallization studies of the Grande Ronde pillow basalts, central Washington. *J. Geol. 90,* 49-78.

Shannon, J. R. Walker, B. M. Carter, R. B. & Geraghty, E. P., 1982: Unidirectional solidification textures and their significance in determining relative ages of intrusion at the Henderson Mine, Colorado. *Geology 10,* 293-297.

Shewmon, P. G. 1969: *Transformations in Metals.* McGraw-Hill.

Swanson, S. E., 1978: Petrology of the Rocklin pluton and associated rocks, western Sierra Nevada, Calif. *Bull. Geol. Soc. Am. 89,* 679-686.

Taubeneck, H. & Poldervaart, A., 1960: Geology of the Elkhorn Mts., Northeast Oregon: 2 Willow Lake intrusion. *Bull. Geol. Soc. Am. 71,* 1295-1322.

Tiller, W. A. Jackson, K. A. Rutter, J. W., & Chalmers, B., 1953: The redistribution of solute atoms during the solidification of metals. *Acta Metall. 1,* 428-437.

Turner, J. S., 1973: *Buoyancy Effects in Fluids.* Cambridge Univ. Press.

Turner, J. S., 1980: A fluid-dynamical model of differentiation and layering in magma chambers. *Nature 285,* 213-215.

Turner, J. S. & Gustavson, L. B., 1978: The flow of hot solutions from vents in the sea floor – some implications for exhalative massive sulfide and other ore deposits. *Econ. Geol., 73,* 1082-1100.

Usselmann, T. M., Lofgren, G. E., Donaldson, C. H. & Williams, R. H., 1975: Experimentally reproduced textures and mineral chemistries of high-titanium mare basalts. *Proc. 6th Lunar Sci. Conf.,* 997-1020.

Voensdreght, C. F., 1983: Crystal morphology of monoclinic potassium feldspars: a qualitative approach with special emphases on the periodic bond chain theory of Hartman & Perdok. *Z. Kristall.*

Wadsworth, W. J., 1960: The ultrabasic rocks of southwest Rhum. *Phil. Trans. Roy. Soc. Lond. Ser.-B 244,* 21-64.

Wager, L. R., Brown, G. M. & Wadsworth, W. J., 1960: Types of igneous cumulates. *J. Petrology 1,* 73-85.

Wager, L. R. & Brown, G. M. 1967: *Layered Igneous Rocks.* Oliver & Boyd.

Wager, L. R. & Deer, W. A., 1939 (re-issued 1962): Geological Investigations in East Greenland, III. The Petrology of the Skaergaard Intrusion, Kangerdlugssuaq, East Greenland. *Medd. om Grønland 105,* No. 4, 1-352.

Walker, D., Kirkpatrick, R. J., Longhi, J., & Hayes, J. F., 1976: Crystallization history of lunar picrite basalt sample 12002: phase equilibia and cooling-rate studies. *Bull. Geol. Soc. Am. 87,* 646-656.

Walker, D., Lesher, C. E., & Hayes, J. F. 1981: Soret separation of lunar liquid. *Proc. Lunar Planet. Sci. Conf. XIIB,* 991-999.

Wilson, J. R & Larsen, S. B, 1982: Discordant layering in the Fongen-Hyllingen basic intrusion. *Nature 299,* 625-626.

Wright, T. L. & Doherty, P. C., 1970: A linear programming and least squares computer method for solving petrological mixing problems. *Bull. Geol. Soc. Am. 81,* 1995-2008.